# Direct Detection, Dimerization, and Chemical Trapping of Dimethyl- and Diphenylstannylene from Photolysis of Stannacyclopent-3-enes in Solution

Ian R. Duffy and William J. Leigh*

Department of Chemistry and Chemical Biology, McMaster University, 1280 Main Street West, Hamilton, ON, Canada L8S 4M1

S *Supporting Information*

ABSTRACT: Dimethyl- and diphenylstannylene (SnMe$_2$ and SnPh$_2$, respectively) have been successfully detected and characterized in solution. The stannylenes were generated by photolysis of 1,1,3-trimethyl-4-phenyl- (**2**) and 3,4-dimethyl-1,1-diphenylstannacyclopent-3-ene (**3**), respectively, which have been shown to extrude the species cleanly and in high (0.6 < Φ < 0.8) quantum yields through trapping studies using dichlorodimethylstannane (Me$_2$SnCl$_2$) as the stannylene substrate. Laser flash photolysis of **2** and **3** in deoxygenated hexanes affords promptly formed transient absorptions assigned to SnMe$_2$ (λ_{max} = 500 nm; ε_{500} = 1800 ± 600 M^{-1} cm^{-1}) and SnPh$_2$ (λ_{max} = 290, 505 nm; ε_{500} = 2500 ± 600 M^{-1} cm^{-1}), respectively, which decay with absolute second-order rate constants within a factor of 2 of the diffusional limit in both cases. The decay of the stannylenes is accompanied by the growth of new transient absorptions ascribable to the corresponding dimers, the structures of which are assigned with the aid of DFT and time-dependent (TD) DFT calculations at the (TD)ωB97XD/6-31+G(d,p)^{C,H,O}-LANL2DZdp^{Sn} level of theory. Dimerization of SnMe$_2$ affords a species exhibiting λ_{max} = 465 nm, which is assigned to the expected Sn=Sn doubly bonded dimer, tetramethyldistannene (Me$_2$Sn=SnMe$_2$, **16a**), in agreement with earlier work. In contrast, the spectrum of the dimer formed from SnPh$_2$ exhibits strong absorptions in the 280−380 nm range and a very weak absorption at 650 nm, on the basis of which it is assigned to phenyl(triphenylstannyl)stannylene (**17b**). The calculations suggest that **17b** is formed via ultrafast rearrangement of a novel phenyl-bridged stannylidenestannylene intermediate (**20**), which can be formed either directly by "endo" dimerization of SnPh$_2$ or by isomerization of the "exo" dimer, tetraphenyldistannene (**16b**); the predicted barriers for these rearrangements are consistent with the experimental finding that the observed product is formed at close to the diffusion-controlled rate. Absolute rate and equilibrium constants are reported for the reactions of SnMe$_2$ and SnPh$_2$ with Me$_2$SnCl$_2$ and methanol (MeOH), respectively, in hexanes at 25 °C.
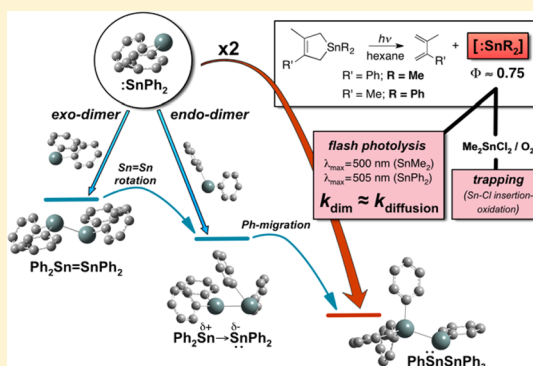
INTRODUCTION

There has been great interest in the synthesis and reactivity of kinetically stabilized dialkyl[1] and diaryl[2] Sn(II) (stannylene) derivatives and in exploring the potential utility of such compounds for applications in catalysis and small-molecule activation.[2j−1] There has also been considerable interest in the synthesis of Sn(II) derivatives stabilized by intra- or intermolecular donor[3] or donor−acceptor[4] interactions. In contrast, relatively little is known about the chemistry of simpler, transient stannylene derivatives such as dimethyl- and diphenylstannylene (SnMe$_2$ and SnPh$_2$, respectively), despite early interest in the preparation and characterization of these molecules.[5]

The reactivity of SnMe$_2$ in solution was studied many years ago by W. P. Neumann and co-workers using both thermolytic and photolytic routes to generate the molecule.[6] More recently, P. P. Gaspar and co-workers examined the reactions of several transient stannylenes (including SnMe$_2$ and the parent diarylstannylene, SnPh$_2$) with dienes, alkyl halides, disulfides, and various other potential substrates in solution at 75−100 °C,

employing 1,1-disubstituted 1-stannacyclopent-3-ene derivatives (**1**) as thermal stannylene precursors.[7] Among other things, these studies showed that simple transient Sn(II) derivatives strongly prefer oligomerization over bimolecular reaction with added substrates, even those that typically show high reactivity toward higher divalent group 14 homologues. Indeed, despite much effort, relatively few reaction types have been identified that proceed rapidly enough to compete productively with oligomerization. The best studied and seemingly most versatile reaction that stannylenes undergo is formal (1+4)-cheletropic cycloaddition with dienes.[2c,d,6h,7,8] The oligomerization process is in itself intriguing, because of the diverse variety of dimeric structures that can potentially be formed;[2g,9] silylenes and germylenes, on the other hand, invariably afford the corresponding doubly bonded (ditetrellene) structures upon dimerization.[9h]

a. R = Me; R' = H
b. R = Me; R' = Me
c. R = n-Bu; R' = H
d. R = t-Bu; R' = H
e. R = Ph; R' = H
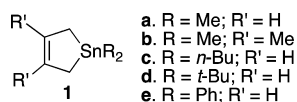
Efforts to detect transient stannylenes directly have focused almost exclusively on the parent dialkylstannylene, $SnMe_2$. The characteristic IR bands of this species, as well as those of its isotopomer $Sn(CD_3)_2$, have been assigned in an argon matrix at 5 K,[10] while more recently $SnMe_2$ has been detected directly in the gas phase[11] and in solution[11b] by (193 nm) laser flash photolysis methods. The gas phase studies, which employed $SnMe_4$[11a] and **1a**[11b] as $SnMe_2$ precursors, examined the stannylene's reactivity with an extensive selection of tetrylene substrates (including alkenes, alkynes, dienes, silyl and germyl hydrides, methanol (MeOH), HCl, alkyl halides, N_2O and SO_2) and characterized it as the least reactive in the series of "heavy carbene" analogues, $SiMe_2$, $GeMe_2$, and $SnMe_2$.[11a] The solution phase study was limited to studying the dimerization of the species and its reactivity with MeOH, with which it was found to complex reversibly but otherwise not react at ambient temperatures.[11b] Various aspects of stannylene reactivity have also been studied computationally.[8d,12] The calculations suggest that, in general, stannylenes should exhibit comparable Lewis acidities to the corresponding Ge(II) and Si(II) derivatives, thus favoring Lewis acid−base complexation as the first step in most of their potential reactions. The calculations further suggest that the general lack of reactivity of stannylenes toward typical tetrylene substrates is due either to prohibitively high reaction barriers for reaction of the intermediate complex (e.g., Si−H insertion)[12f] or to unfavorable overall reaction thermochemistries (e.g., (1+2)-cycloadditions to C−C multiple bonds).[8d,12a,c,f]

Our earlier study of $SnMe_2$ in solution employed the stannacyclopent-3-ene derivative **1b** as the stannylene precursor, but the necessity of employing 193 nm light to excite the molecule severely restricted the scope of our studies of the stannylene's reactivity. Expanding the scope of the study to include a greater variety of substrates (alkenes, alkynes, amines, sulfides, ethers, etc.) requires the development of a precursor that absorbs at longer wavelengths.

Given the suitability of **1b** as a precursor to $SnMe_2$ for solution phase studies, the fact that 3-phenylgermacyclopent-3-ene derivatives are efficient 248 nm precursors to transient Ge(II) derivatives such as $GeMe_2$[13] and GeH_2[14] in solution and the recent development by Gaspar's group of a general methodology for the synthesis of stannacyclopent-3-ene derivatives,[7] we were encouraged to synthesize the phenylated $SnMe_2$ precursor **2** and examine its photochemistry, with the goals of detecting $SnMe_2$ in solution by 248 nm flash photolysis and studying its reactivity in greater detail than has so far been possible. Gaspar and co-workers reported the synthesis of a closely related 3-phenylstannacyclopent-3-ene derivative[7] via a procedure that appeared amenable to modification.
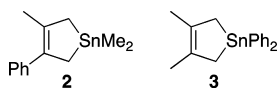

A second goal was to examine the photochemistry of 3,4-dimethyl-1,1-diphenylstannacyclopent-3-ene (**3**),[7] a potential photochemical precursor to the prototypical diarylstannylene, $SnPh_2$. Given that the corresponding germanium homologue of **3** photoextrudes $GePh_2$ in high chemical and quantum yields,[15] we strongly suspected we could generate $SnPh_2$ in similarly

high yields by photolysis of the tin derivative (**3**), thus enabling the direct detection and study of the prototypical diarylstannylene for the first time by time-resolved spectroscopic methods.

In this paper, we thus report the results of a study of the photochemistry of **2** and **3** in hydrocarbon solvents by steady-state and laser flash photolysis methods. Photolysis of the two compounds in solution is shown to afford products consistent with the formation of the corresponding stannylenes as the primary tin-containing photoproducts, through chemical trapping experiments with dichlorodimethylstannane (Me_2SnCl_2) as the trapping agent.[6e] Laser photolysis of the two compounds affords readily detectable transient absorptions that are assigned to the respective stannylenes on the basis of their UV−vis spectra, dimerization behavior, and reactivity toward Me_2SnCl_2 and methanol (MeOH), for which absolute rate or equilibrium constants are also reported. Density functional theory (DFT) calculations at the ωB97XD/6-31+G(d,p)^{C,H,O}-LANL2DZdp^{Sn} level have also been carried out, to support the transient spectral assignments and to assist in the interpretation of the experimental results for the oligomerization chemistry of $SnMe_2$ and $SnPh_2$.

■ RESULTS AND DISCUSSION

Compounds **2** and **3** were prepared by reaction of the magnesium complexes of 2-methyl-3-phenyl-1,3-butadiene (**4a**) and 2,3-dimethyl-1,3-butadiene (**4b**), respectively, with the appropriate dichlorostannane (Me_2SnCl_2 for **2** and Ph_2SnCl_2 for **3**; see eq 1), using procedures adapted from those reported


(1)

4
a. R = Ph
b. R = Me
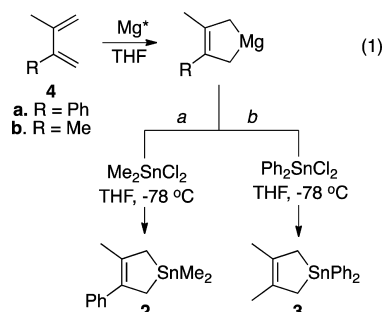
by Gaspar and co-workers.[7] The two compounds were obtained in overall (crude) yields of 30−50% and were each purified by repeated distillation and(or) column chromatography to ≥98% purity (as estimated by ^1H NMR spectroscopy) prior to being used in photochemical experiments.

Stannacyclopent-3-ene Photochemistry: Trapping of Transient Stannylenes. Steady-state photolysis experiments were carried out in quartz NMR tubes with low-pressure mercury lamps (254 nm), on C_6D_{12} solutions of **2** and **3** (ca. 0.04 M) containing Si_2Me_6 as internal standard, both alone and in the presence of 0.03−0.04 M Me_2SnCl_2. Neumann and co-workers identified this reagent as an efficient substrate for $SnMe_2$, with which it reacts via formal Sn−Cl bond insertion to afford the corresponding 1,2-dichlorodistannane as the primary product.[6e] Although Me_2SnCl_2 has limited solubility in cyclohexane, it has the advantage of being transparent at 254 nm, unlike most of the other potential stannylene substrates that earlier studies suggested might be useful as trapping agents.[6a,h,7] The photolyses were monitored at selected time intervals throughout the photolysis by ^1H NMR spectroscopy and taken to a maximum conversion of ca. 25% in

stannacyclopentene; product yields were calculated from the initial slopes of concentration vs time plots for the various products relative to the initial slopes of the corresponding plots for **2** or **3**. This was supplemented with the ^{119}Sn{^{1}H} NMR spectra of the photolyzed mixtures at the end of each experiment, to further aid in product identification. Most photolyses were carried out both with and without deaeration of the solution prior to photolysis, as the presence of air led to significantly higher photolysis rates (particularly with **3**) owing to oxidation of the primary tin-containing photoproducts to the corresponding stannoxanes, which are nonabsorbing and/or nonphotoreactive under the conditions of our experiments.

Steady-state photolysis of **2** as a deaerated 0.04 M solution in cyclohexane-d_{12} led to the efficient consumption of the stannacyclopentene and the formation of diene **4a**, in addition to a collection of compounds exhibiting ^{1}H and ^{119}Sn NMR resonances in the ranges characteristic of [SnMe$_2$]$_n$ oligomers (Figure S1).[6g,7] Exposure of the photolyzed solution to air resulted in the formation of a colorless precipitate, as expected for these materials.[6g,7] Chemical yields of (89 ± 5)% and (98 ± 5)% for the major [SnMe$_2$]$_n$ oligomer and diene **4a**, respectively, were determined from the relative slopes of the concentration vs time plots for the products relative to consumed **2** (eq 2; Figure S2).

$$\text{(2)}$$
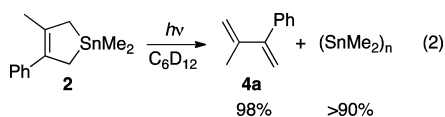
In contrast, photolysis of a deaerated solution of **3** in C$_6$D$_{12}$ under similar conditions resulted in the immediate precipitation of a solid and the development of a yellow color that deepened with continued irradiation. ^{1}H NMR spectra of the mixture (Figure S3) indicated that **3** was consumed with the concomitant formation of diene **4b** and small amounts of at least three compounds whose spectral characteristics and reactivity are consistent with (SnPh$_2$)$_n$ oligomers (eq 3). Two

$$\text{(3)}$$
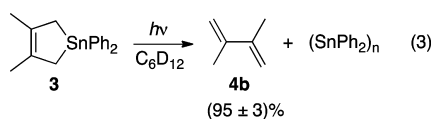
of the three product-derived multiplets that were present in the aromatic region of the NMR spectrum of the photolysate (Figure S3) disappeared after allowing the solution to stand for 18 h in the dark, most likely due to oxidation resulting from gradual contact with air. The multiplet that remained was identified as due to dodecaphenylcyclohexastannane (c-Sn$_6$Ph$_{12}$), by spiking the mixture (in benzene-d_6) with an authentic sample. The concentration vs time plot for this compound (Figure S4a) exhibits positive curvature, consistent with it being derived (at least partially) from secondary photolysis; the initial slope of the plot indicates an upper limit of ca. 10% for the chemical yield relative to consumed **3** (on a per-SnPh$_2$ unit basis). The consumption of **3** and formation of **4b** proceeded significantly faster upon irradiation of an air-saturated solution under similar conditions (Figure S4b), as did the precipitation of insoluble material, and the solution remained colorless throughout the photolysis up to ca. 8% conversion of **3**. No other products could be detected (by NMR) under the conditions employed for the analysis.

Photolysis of a deaerated 0.04 M solution of **2** in C$_6$D$_{12}$ containing Me$_2$SnCl$_2$ (0.033 M) resulted in the consumption of **2** and the formation of **4a** (98 ± 9%) along with three major tin-containing products (eq 4), which were identified as 1,2-

$$\text{(4)}$$
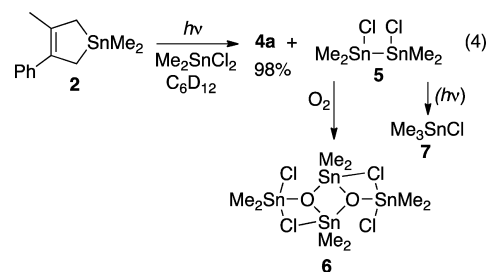
dichlorotetramethyldistannane (**5**, δ_H 0.807 ($^2J_{SnH}$ = 53.5 Hz, $^3J_{SnH}$ = 13.0 Hz), δ_{Sn} 99.2; 51 ± 6%),[16] the association dimer of 1,2-dichlorotetramethyldistannoxane (**6**, δ_H 1.049 and 1.144; δ_{Sn} −63.3 and −125.4; 39 ± 6%),[17] and chlorotrimethylstannane (**7**, δ_H 0.524; 9 ± 2%); Figure S5 shows ^{1}H NMR spectra of the mixture before and after photolysis to ca. 20% conversion of **2**. Concentration vs time plots for **2**, **4a**, and **5−7** are shown in Figure 1; that for **7** exhibits upward curvature,
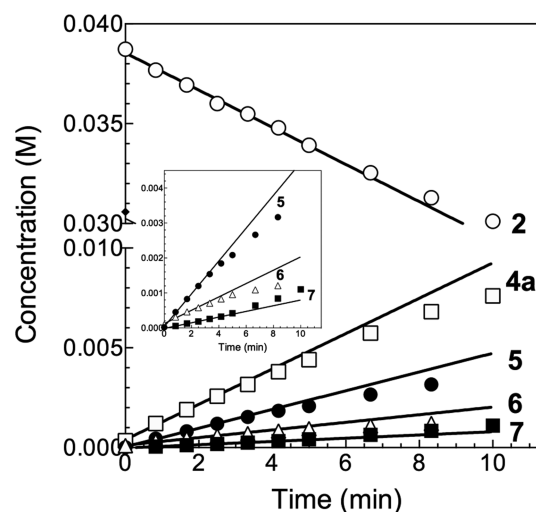

Figure 1. Concentration vs time plots for the photolysis of a deaerated 0.04 M solution of **2** in C$_6$D$_{12}$ containing Me$_2$SnCl$_2$ (0.031 M). The initial slopes of the plots for the various components of the reaction mixture, determined from the first five data points in each case, are **2**, −0.93 ± 0.09; Me$_2$SnCl$_2$ (not shown), −0.89 ± 0.07; **4a**, 0.89 ± 0.07; **5** (ClMe$_2$SnSnMe$_2$Cl), 0.47 ± 0.03; **6** (ClMe$_2$SnOSnMe$_2$Cl)$_2$, 0.19 ± 0.04; **7** (Me$_3$SnCl), 0.08 ± 0.01 (units, mM min^{-1}). The inset shows an expansion of the plots for **5**, **6**, and **7**.

consistent with it being formed as a secondary photolysis product of distannane **5**.[6g] Compound **6** is ascribed to oxidation of **5** by residual oxygen in the solvent.[18]

Indeed, photolysis of an undeaerated solution of **2** and Me$_2$SnCl$_2$ in C$_6$D$_{12}$ produced **4a** and **6** in close to quantitative yields and only trace amounts of **5** and **7** during the initial few minutes of irradiation. Upon continued photolysis the formation of **6** slowed significantly and was supplanted by the formation of **5** and **7**, which proceeded at a combined total rate roughly equal to the initial rate of formation of **6**. The concentration vs time plots from the experiment are shown in Figure 2; it should be noted that the break-points in the plots for the three tin-containing products (see inset) occur at the
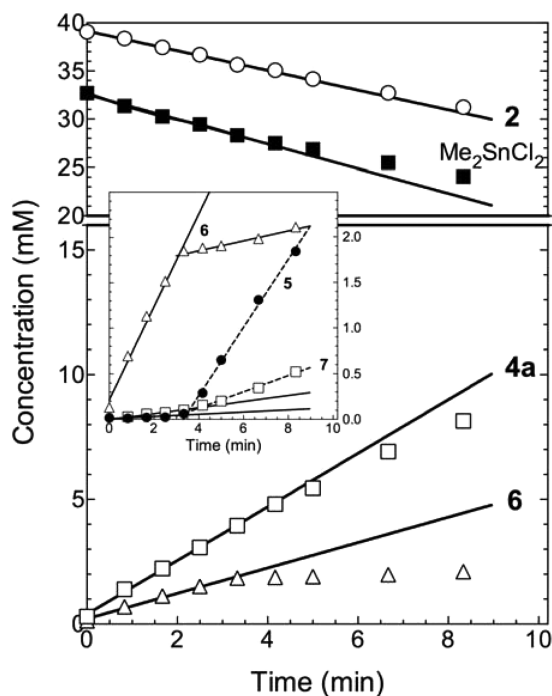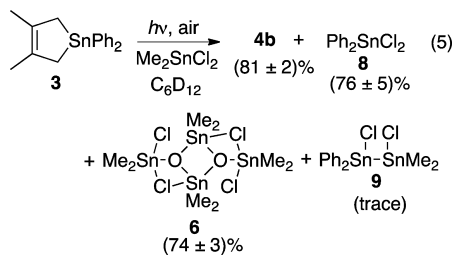
Figure 2. Concentration vs time plots for the photolysis of a solution of **2** (ca. 0.04 M) and Me$_2$SnCl$_2$ (0.033 M) in C$_6$D$_{12}$, which was saturated with air prior to irradiation. The inset shows an expanded plot, detailing the formation of dichlorodistannane **5**, distannoxane dimer **6**, and Me$_3$SnCl (**7**) with photolysis time. The initial slopes, determined from the first five data points in each of the plots, are (in units of mM min^{-1}) **2**, -1.02 ± 0.04; Me$_2$SnCl$_2$, -1.28 ± 0.06; **4a**, 1.08 ± 0.04; **5**, 0.012 ± 0.005; **6**, 0.51 ± 0.03 (<4 min); **7**, 0.033 ± 0.003 (<4 min). The slopes of the second half (>4 min) of the plots for **5**–**7** are **5**, 0.37 ± 0.02; **6**, 0.055 ± 0.007; **7**, 0.10 ± 0.01.

Figure 3. Concentration vs time plots for the photolysis of an undeaerated 0.04 M solution of **3** in C$_6$D$_{12}$ containing 0.037 M Me$_2$SnCl$_2$. The initial (≤ 2.5 min) slopes of the plots (in mM min^{-1}) are **3**, -0.91 ± 0.01; Me$_2$SnCl$_2$, -1.84 ± 0.07; **4b**, 0.74 ± 0.01; **8**, 0.69 ± 0.04; **6**, 0.34 ± 0.02; **9** (≥ 3.3 min), 0.08 ± 0.04; **13a** (≥ 3.3 min), 0.036 ± 0.003. No attempt was made to replenish the air in the photolysate as the experiment proceeded.

point where the concentration of **6** is roughly 80% of the (initial) oxygen concentration in air-saturated cyclohexane (ca. 2.4 mM[19]). The presence of air caused a barely significant increase in the initial rates of photolysis of **2** and formation of **4a** compared to those in deaerated solution, which allows the conclusion that O$_2$ (at a concentration of ca. 3 mM or less) interacts only with the primary photoproducts and does not interact with the reactive excited state of the stannacyclopentene (**2**).

Photolysis of an undeaerated 0.04 M solution of **3** in C$_6$D$_{12}$ containing Me$_2$SnCl$_2$ (0.037 M) afforded diene **4b**, Ph$_2$SnCl$_2$ (**8**), and distannoxane dimer **6** as the major products at low

(<6%) conversions of **3** (eq 5); Figure S6 shows representative ^{1}H NMR spectra recorded throughout the photolysis, while the concentration vs time plots from which the initial yields were calculated are shown in Figure 3. The plots exhibit good linearity over the first 2.5 min of photolysis and also reveal that
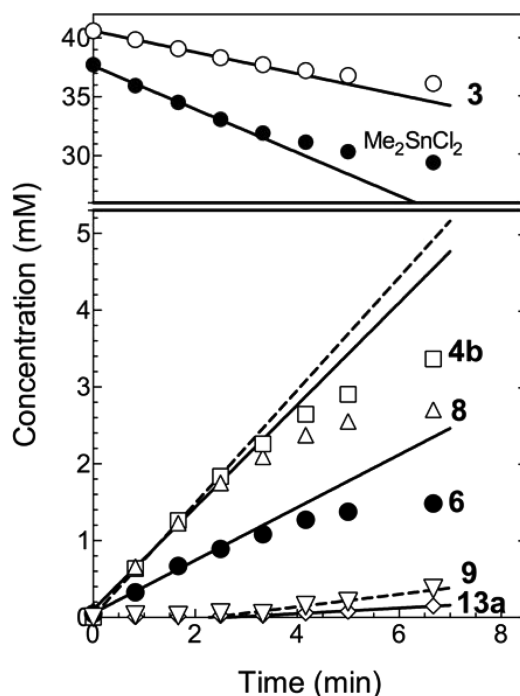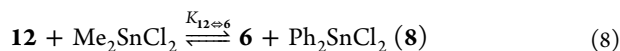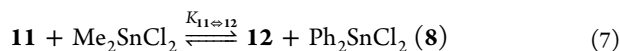
the consumption of Me$_2$SnCl$_2$ proceeds at roughly twice the rate of consumption of **3** during the initial (2.5 min) photolysis period, as expected considering that **6** is a major product of the reaction. Continuation of the photolysis past ca. 5% conversion of **3**—and the point where the O$_2$ concentration had been reduced by 80–90% from its initial level (*vide supra*)—resulted in significant yellowing of the solution, sharp downward curvature in the concentration vs time plots for **4b**, **6**, and **8**, and the enhanced growth of several of the minor product resonances in the ^{1}H NMR spectra. One of the minor product peaks was a singlet at δ 0.895, which we assign tentatively to 1,2-dichlorodistannane **9**, the expected primary product of insertion of SnPh$_2$ into a Sn–Cl bond of the substrate.

A reasonable mechanism for the formation of **6** and **8** in this experiment involves air-oxidation of 1,2-dichlorodistannane **9** to afford the corresponding 1,3-dichlorodistannoxane (**10**), which dimerizes to the corresponding association dimer (**11**) and then liberates **8** by exchange with excess Me$_2$SnCl$_2$ (eq 6); exchange processes in compounds of this type are known to proceed rapidly in solution at ambient temperatures.[20] Assuming that the equilibration of **6**, **11**, and the intermediate cyclodistannoxane (**12**) is rapid and that the three species have similar thermodynamic stabilities under the conditions of our experiments, then the mechanism predicts that the mixed dimer (**12**) should be present at 10–20% the concentration of **6** at the highest conversion (of **3**) examined, where **6**, **8**, and Me$_2$SnCl$_2$ are present at concentrations of ca. 1.5, 2.7, and 29 mM, respectively (see Figure 3). Indeed, the ^{1}H NMR spectrum of the photolyzed mixture shows a weak doublet at δ 8.09 (Figure S6C), which is consistent with the presence of **12** as a minor component in the photolysate;[21] integration of

$$\text{(6)}$$

$$\text{(9)}$$
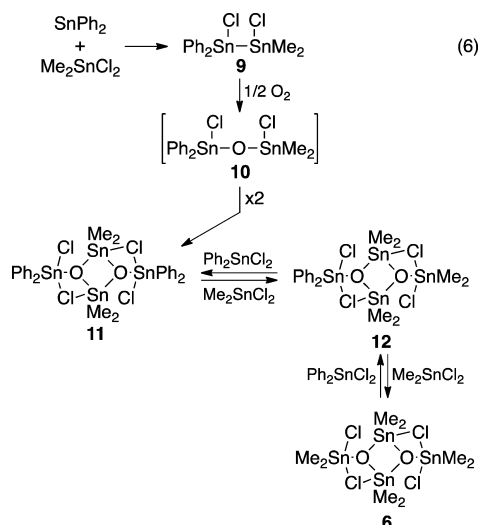
the spectrum indicates that **12** and **6** are present in relative concentrations of $[\mathbf{12}]:[\mathbf{6}] = 0.14 \pm 0.02$. Addition of aliquots of Ph_2SnCl_2 (**8**) to the photolysate caused an increase in the intensity of a weaker doublet at δ 8.06 (relative to the δ 8.09 doublet), which we tentatively assign to cyclodistannoxane **11**, formed by exchange of **8** with the exocyclic Me_2SnCl_2 moiety in **12**.

Additional support for these assignments was obtained by analysis of the ^{1}H NMR spectra of a series of mixtures of Me_2SnCl_2, **8**, and authentic **6** in $CDCl_3$ solution. These spectra also showed two doublets in the aromatic region assignable to **11** (δ 8.03) and **12** (δ 8.06), in relative intensities (i.e., **11**:**12**) that increased as the $[\mathbf{8}]:[Me_2SnCl_2]$ ratio was increased (see Supporting Information). Analysis of the compositions of four different synthetic mixtures according to the expressions for the equilibrium constants for interconversion of **11**, **12**, and **6** (eqs 7, 8) afforded values of $K_{12 \Leftrightarrow 6} = 0.46 \pm 0.03$ and $K_{11 \Leftrightarrow 12} = 0.81 \pm 0.14$ in $CDCl_3$ at 22 °C (see Figure S7). The values predict that at the highest conversion of **3** achieved in the photolysis with 0.037 M Me_2SnCl_2 in undeaerated C_6D_{12} (Figure 3), cyclodistannoxanes **6** and **12** should be present in the ratio $[\mathbf{12}]:[\mathbf{6}] \approx 0.20$, given the relative concentrations of **8** and Me_2SnCl_2 at this point ($[Me_2SnCl_2]:[\mathbf{8}] \approx 10.7$) and assuming a negligible solvent effect on the equilibrium constants. Considering the uncertainties, the estimate is in reasonable agreement with the value determined from the ^{1}H NMR spectrum of the photolysate.

$$\mathbf{11} + Me_2SnCl_2 \xrightleftharpoons{K_{11 \Leftrightarrow 12}} \mathbf{12} + Ph_2SnCl_2 \ (\mathbf{8}) \qquad (7)$$

$$\mathbf{12} + Me_2SnCl_2 \xrightleftharpoons{K_{12 \Leftrightarrow 6}} \mathbf{6} + Ph_2SnCl_2 \ (\mathbf{8}) \qquad (8)$$

Photolysis of a deaerated[22] solution of **3** in C_6D_{12} containing Me_2SnCl_2 (0.035 M) resulted in rapid yellowing of the solution and the appearance of the singlet at δ 0.895 assigned above to distannane **9** (Figure S8), which was the major Sn-containing product over the first 3% conversion of **3**. It was formed in an estimated yield of (42 ± 10)% along with diene **4b** (ca. 79%), **6** (ca. 24%), and **8** (ca. 25%) (eq 9), based on the relative slopes of the concentration vs time plots between 0% and 3% conversion of **3** (Figure 4). At conversions greater than 3% the plot for **9** curved sharply downward, indicating that secondary photolysis of **9** competes with the primary photolysis of **3** as the former builds up in solution; several minor products were
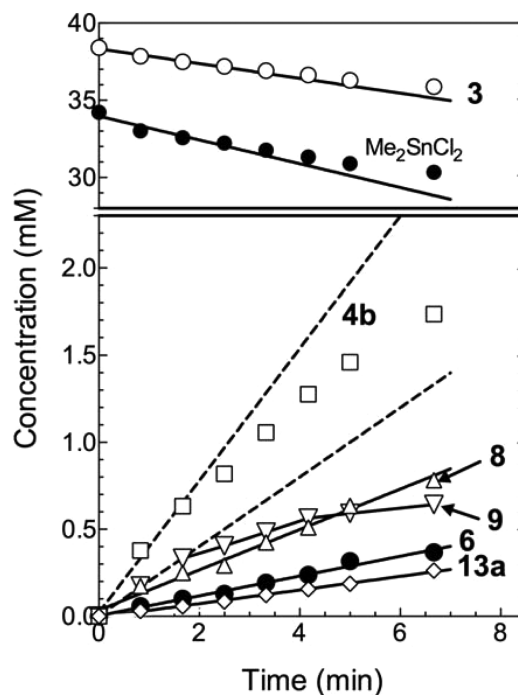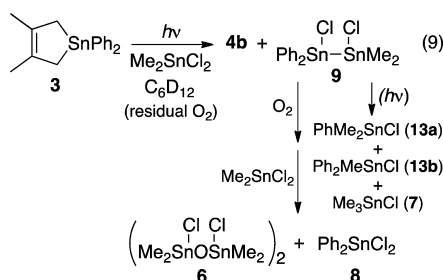

Figure 4. Concentration vs time plots for the photolysis of a deaerated[21] 0.038 M solution of **3** in C_6D_{12} containing Me_2SnCl_2 (0.034 M). The initial slopes of the plots (in mM min^{-1}) are **3**, -0.48 ± 0.05; Me_2SnCl_2, -0.77; **4b**, 0.38 ± 0.04; **6**, 0.057 ± 0.003; **8**, 0.12 ± 0.01; **9**, 0.199 ± 0.006; **13a**, 0.039 ± 0.001; **13b** (not shown), 0.022 ± 0.002; **7** (not shown), 0.017 ± 0.001.

also observed in this experiment, in enhanced yields compared to those in undeaerated solution. Two of the minor products were identified as $Me_2PhSnCl$ (**13a**; 8%) and $MePh_2SnCl$ (**13b**; 5%) on the basis of their ^{1}H NMR spectra (Figure S8),[23] while **7** (3.5%) was identified by comparison with an authentic sample. These compounds, along with $(SnMe_2)_n$ oligomers (which were also tentatively identified in the spectrum) and a portion of the amount of **8** that is formed, are the products expected from photolysis of diaryldistannane **9**, which can be expected to absorb quite strongly at 254 nm.[6f] The formation of **6** and the majority of **8** that is formed can be ascribed to incomplete deaeration of the solution prior to photolysis.

Quantum yields for the formation of **6** from photolysis of **2** and **3** as air-saturated, 0.04 M solutions in C_6D_{12} containing 0.03−0.04 M Me_2SnCl_2 were determined using the photolysis of 3,4-dimethyl-1,1-diphenylgermacyclopent-3-ene **14** ($\Phi_{16} = 0.55 \pm 0.07$ in methanolic C_6D_{12};[15] eq 10) as actinometer. The
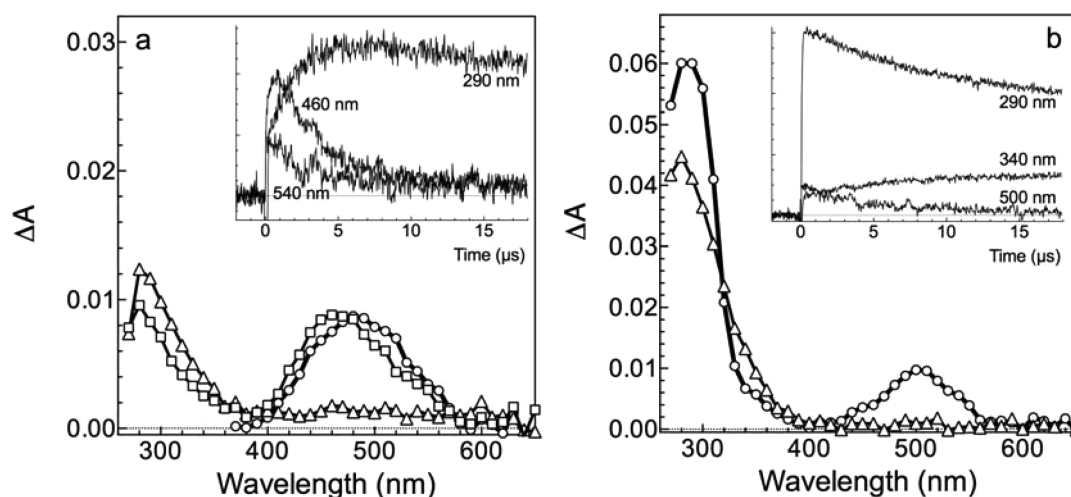
$$\text{(10)}$$
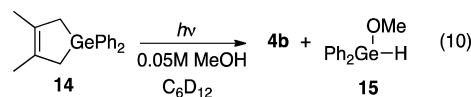
Figure 5. Transient UV−vis absorption spectra from laser flash photolysis of rapidly flowed solutions of (a) **2** (2×10^{-4} M) and (b) **3** (7×10^{-4} M) in anhydrous hexanes at 25 °C. The spectra in (a) were recorded 0.19−0.26 μs (○), 0.70−0.80 μs (□), and 17.2−17.3 μs (△) after the laser pulse, while those in (b) were recorded 0.35−0.45 μs (○) and 17.1−17.3 μs (△) after the pulse; the insets show absorbance vs time profiles recorded at selected wavelengths in the two spectra. The spectra in (a) were recorded at reduced laser intensity in order to maximize the temporal resolution between the primary and secondary product spectra.

values obtained for **2** ($\Phi_{SnMe2} = 0.78 \pm 0.10$) and **3** ($\Phi_{SnPh2} = 0.61 \pm 0.09$) were calculated from the initial slopes ($\times 2$) of the concentration vs time plots for **6** relative to that of **15** from the photolysis of the actinometer (Figure S9). In the case of **3**, the value of Φ_{SnPh2} obtained is the same regardless of which of the two major Sn-containing products (**6** or **8**) is used for the calculation, as expected (Figure S9b,c).

Direct Detection of Transient Stannylenes by Laser Flash Photolysis. Laser flash photolysis experiments were carried out with rapidly flowed, deoxygenated solutions of **2** and **3** in anhydrous hexanes, using the pulses from a KrF excimer laser (248 nm, 95−105 mJ, ca. 25 ns) for excitation. In both cases laser photolysis gave rise to readily detectable transient absorptions throughout the 270−600 nm spectral range, one set of absorptions that were formed during the laser pulse (and are thus assignable to a primary photoproduct), and a second set that grew in concomitantly with the decay of the primary absorptions and are thus assignable to secondary products formed via (ground-state) reaction of the primary transient; with **2**, the decay of the secondary products was accompanied by the growth of a third set of absorptions, as we found in the earlier study with **1b** as SnMe$_2$ precursor.[11b] In both cases, but particularly with **3**, the quality of the signals tended to degrade steadily throughout the course of an experiment due to the gradual appearance of periodic spikes in the absorbance vs time profiles. These result from the buildup of particulate material on the inner walls of the sample cell, which worsens as the experiment progresses.[24] They did not interfere with the recording of transient UV−vis spectra and generally did not compromise the determination of decay rate coefficients from the absorbance vs time profiles.

The decay of the prompt absorption produced upon laser photolysis of **2** (monitored at 540 nm to avoid overlap with the secondary absorption) was found to proceed with clean second-order kinetics and rate coefficient $2k/\varepsilon_{540} = (3.0 \pm 0.3) \times 10^7$ cm s^{-1}, in good agreement with the value reported in the earlier solution phase study.[11b] Figure 5a shows representative transient absorption spectra and absorbance−time profiles obtained with this compound. As in the earlier work, we assign the prompt absorption to SnMe$_2$, the secondary absorption

centered at $\lambda_{max} \approx 465$ nm to tetramethyldistannene (Me$_2$Sn══SnMe$_2$, **16a**), and the tertiary absorption below 320 nm to a product of further reaction of the distannene.[11b] The apparent λ_{max} value of 490 nm for SnMe$_2$ is in acceptable agreement with the earlier reported value ($\lambda_{max} = 500$ nm), the apparent blue shift occurring most likely because the higher transient concentrations achieved in the present work result in faster second-order decays, which compromises our ability to isolate temporally the spectrum of the prompt transient from that of the dimerization product (**16a**). The value of $\lambda_{max} = 465$ nm observed in the present work for the absorption maximum of the latter species and the time scale over which it decays are also in good agreement with the previously reported data.[11b]
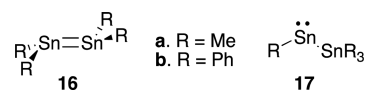
Laser photolysis of **3** also led to at least two sequentially formed transient products. The initially formed species exhibits absorption bands centered at $\lambda_{max} = 290$ and 505 nm that decay together over ca. 20 μs, leaving behind a longer lived species exhibiting a broad absorption with $\lambda_{max} < 280$ nm that tails out to ca. 400 nm (Figure 5b). The 505 nm species (monitored at 500 nm) decays with clean second-order kinetics and rate coefficient $2k/\varepsilon_{500} = (1.3 \pm 0.2) \times 10^7$ cm s^{-1}, consistent with dimerization as the main mode of decay, and we thus assign it to SnPh$_2$. Notably, the absorption maximum of the species is blue-shifted compared to those typical of sterically hindered diarylstannylenes,[2a,d,25] which is a feature that is also shared by diarylsilylene and -germylene systems.[15,26] An absorbance vs time profile recorded at 340 nm, on the long wavelength tail of the broad 280 nm absorption, consists of a growth that occurs over a time scale similar to the decay of the 505 nm SnPh$_2$ absorption (Figure 5b), suggesting it is associated with the product of the dimerization reaction. Importantly, there is no evidence of a strong product absorption anywhere throughout the 450−600 nm spectral range, the range characteristic of tetraaryldistannenes.[25a,27] We thus conclude that, in contrast to the behavior of SnMe$_2$ (*vide supra*) and the higher

diphenyltetrylenes, SiPh$_2$[26b,28] and GePh$_2$,[15] the dimerization of SnPh$_2$ does *not* afford the corresponding (Sn=Sn) doubly bonded dimer (**16b**) in detectable amounts, but rather some other Sn$_2$Ph$_4$ isomer, formed perhaps via (rapid) isomerization of **16b**; the most reasonable candidate, based on computational[29] and experimental[2g] precedent, is phenyltriphenylstannylstannylene (**17b**). The latter can be expected to exhibit a very weak n → 5p absorption in the 600−800 nm range of the visible spectrum,[25a,30] which is unfortunately in a region of relatively low sensitivity for our spectrometer. Nevertheless, careful probing in this spectral range did reveal a barely detectable product absorption centered apparently at $\lambda_{\text{max}} \approx$ 650 nm, which appeared to grow in over a time scale similar to the growth of the absorption at 340 nm (see Figure S10). The result cannot be considered conclusive, but is nevertheless consistent with the tentative assignment of the observed dimer to stannylstannylene **17b**. The assignment is also supported by the results of computational studies of the Sn$_2$Ph$_4$ potential energy surface, as discussed later in the paper.

The steady-state photolysis experiments suggest that both stannylenes can be trapped efficiently by Me$_2$SnCl$_2$ (*vide supra*), so we carried out transient quenching experiments with **2** and **3** using the dichlorostannane as the substrate, monitoring the prompt absorptions assigned to the stannylenes (at 530 and 500 nm, respectively) as a function of Me$_2$SnCl$_2$ concentration. Indeed, addition of submillimolar concentrations of Me$_2$SnCl$_2$ in hexanes caused the decays to accelerate and proceed with clean pseudo-first-order kinetics in both cases, in a manner consistent with irreversible reaction. Accompanying this was a reduction in the intensities of the signals due to the dimerization products, indicating dimerization is suppressed in the presence of the added substrate, as might be expected. Plots of the pseudo-first-order rate constants for decay of the prompt absorptions (k_{decay}) vs Me$_2$SnCl$_2$ concentration according to eq 11 were both linear (see Figure 6), consistent with an overall second-order reaction. The slopes of the plots afford bimolecular rate constants of $k_Q = (1.9 \pm 0.3) \times 10^{10}$ and
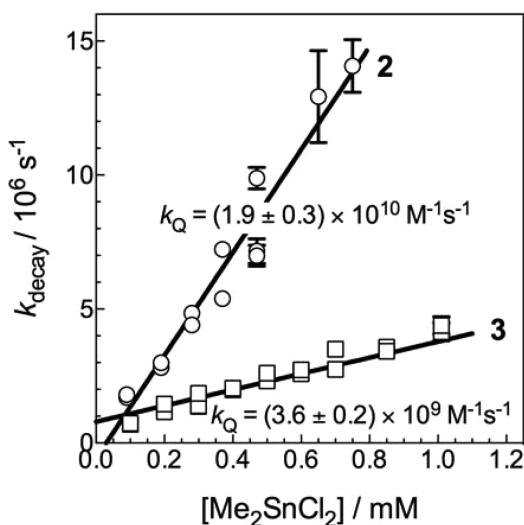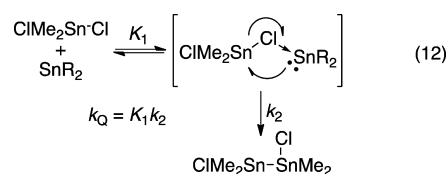

Figure 6. Plots of k_{decay} vs substrate concentration for the stannylene absorptions from laser photolysis of hexanes solutions of (a) **2** (○) and (b) **3** (□) containing varying concentrations of Me$_2$SnCl$_2$ at 25 °C. The monitoring wavelengths were 530 and 500 nm for **2** and **3**, respectively. The solid lines are the linear least-squares fits of the data to eq 11.

$(3.6 \pm 0.2) \times 10^9$ M^{-1} s^{-1} for the reactions of Me$_2$SnCl$_2$ with SnMe$_2$ and SnPh$_2$, respectively. A transient spectrum recorded with **2** in hexanes containing 0.3 mM Me$_2$SnCl$_2$, where the lifetime of SnMe$_2$ is reduced to ca. 230 ns and dimerization is suppressed almost completely, exhibited λ_{max} = 500 nm, which is in excellent agreement with the earlier reported spectrum of SnMe$_2$ in hexanes solution.[11b] No other transient products could be detected in the experiment.
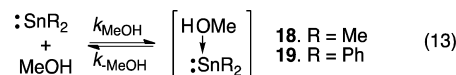
$$k_{\text{decay}} = k_0 + k_Q[\text{Q}] \tag{11}$$

The kinetic data for the reactions with the dichlorostannane are consistent with a two-step mechanism involving reversible Lewis acid−base complexation of the stannylene with the halostannane, followed by insertion of the Sn(II) site into the (complexed) Sn−Cl bond (eq 12). The mechanism is analogous to that for Si−Cl bond insertions by silylenes, which has been studied extensively by Kira and co-workers.[31]

$$
\begin{array}{c}
\text{ClMe}_2\text{Sn-Cl} \\
+ \\
\text{SnR}_2
\end{array}
\overset{K_1}{\rightleftharpoons}
\left[\text{ClMe}_2\text{Sn}\overset{\text{Cl}}{\underset{}{\cdots}}\text{:SnR}_2 \right]
\tag{12}
$$

$$k_Q = K_1 k_2 \qquad\qquad \downarrow k_2$$

$$
\underset{\text{ClMe}_2\text{Sn-SnMe}_2}{\overset{\text{Cl}}{|}}
$$

The extinction coefficients of SnMe$_2$ and SnPh$_2$ at 500 nm were determined by benzophenone actinometry, in conjunction with the photoproduct quantum yields determined in the previous section (see Figure S11).[32] The values obtained—ε_{500} = 1800 ± 600 M^{-1} cm^{-1} for SnMe$_2$ and ε_{500} = 2500 ± 600 M^{-1} cm^{-1} for SnPh$_2$—are in the range typical of the n → p absorption bands of dialkyl- and diaryltetrylenes (MR$_2$; M = Si, Ge, or Sn) in solution.[1c,f,2h,13,15,25,33] Use of these data with the second-order decay rate coefficients reported above affords k_{dim} = $(1.4 \pm 0.4) \times 10^{10}$ M^{-1} s^{-1} for the second-order rate constant for dimerization of SnMe$_2$[34] and k_{dim} = $(1.6 \pm 0.4) \times 10^{10}$ M^{-1} s^{-1} as the corresponding value for SnPh$_2$. It can thus be concluded that the dimerization of both stannylenes proceeds with absolute second-order rate constants that are very close to the diffusional limit in solution.

A final set of laser photolysis experiments was carried out using methanol (MeOH) as the substrate, a reagent found in our earlier study to react with SnMe$_2$ *reversibly* to form a transient product exhibiting $\lambda_{\text{max}} \approx$ 360 nm, which was assigned to the Me$_2$Sn−O(H)Me Lewis acid−base complex (**18**; eq 13).[11b] Indeed, addition of 0.1−1.5 mM MeOH to hexanes

$$
\begin{array}{c}
\text{:SnR}_2 \\
+ \\
\text{MeOH}
\end{array}
\underset{k_{-\text{MeOH}}}{\overset{k_{\text{MeOH}}}{\rightleftharpoons}}
\left[\underset{\text{:SnR}_2}{\overset{\text{HOMe}}{\underset{}{\downarrow}}} \right]
\quad
\begin{array}{l}
\textbf{18.}\ \text{R = Me} \\
\textbf{19.}\ \text{R = Ph}
\end{array}
\tag{13}
$$

solutions of **2** caused closely analogous behavior to what was observed in the earlier study;[11b] the intensities of the signals due to both SnMe$_2$ and Sn$_2$Me$_4$ were reduced in a manner consistent with a moderately favorable, reversible reaction of the alcohol with the stannylene,[35] giving rise to a new transient product exhibiting a similar lifetime to the stannylene (as expected if the complex is in mobile equilibrium with the free stannylene) and a UV−vis spectrum centered at λ_{max} = 355 nm (Figure S12a). A plot of the relative stannylene signal intensities as a function of MeOH concentration according to eq 14, where $(\Delta A_0)_0$ and $(\Delta A_0)_Q$ are the initial signal intensities (at 530 nm) in the absence and presence of the substrate at concentration [Q] and K_{MeOH} (= $k_{\text{MeOH}}/k_{-\text{MeOH}}$) is
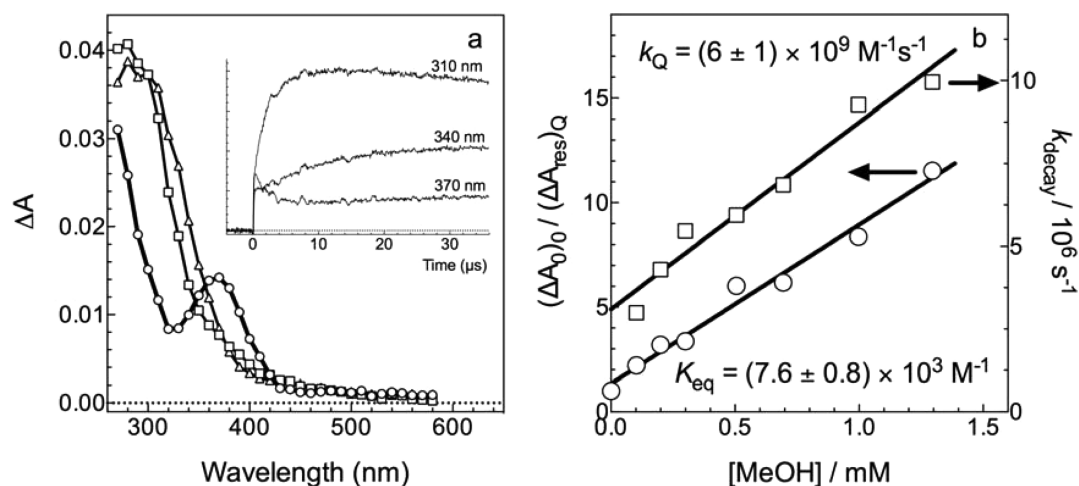
Figure 7. (a) Time-resolved UV−vis spectra from laser photolysis of SnPh$_2$ precursor **3** in hexanes containing 0.025 M MeOH, 0.26−0.38 μs (○), 4.93−5.18 μs (□), and 35.3−35.7 μs (△) after the laser pulse (25 °C), and absorbance−time profiles at selected wavelengths (inset). (b) Plots of k_{decay} (□) and $(\Delta A_0)_0/(\Delta A_0)_Q$ (○) of the SnPh$_2$ absorption (at 500 nm) vs [MeOH], in hexanes solution at 25 °C; the solid lines are the linear least-squares fits of the data to eqs 11 and 14, respectively.

the equilibrium constant, was linear (Figure S12b) with slope $K_{MeOH} = (2.4 \pm 0.2) \times 10^3$ M^{-1}. The value is larger than the earlier reported value by a factor of about 2,[11b] but can be considered to be the more accurate of the two determinations. Interestingly, a time-resolved spectrum recorded with **2** in hexanes containing 0.025 M MeOH exhibited an absorption band centered at $\lambda_{max} = 335$ nm, blue-shifted significantly compared to that obtained in the presence of 7 mM of the alcohol. This may be the result of the formation of dicoordinate complexes (i.e., SnMe$_2$−(MeOH)$_2$) at the higher alcohol concentration.[36] It should be noted that distannene (**16a**) formation appears to be suppressed in the presence of the alcohol.

$$(\Delta A_0)_0/(\Delta A_0)_Q = 1 + K_{eq}[Q] \qquad (14)$$

A transient UV−vis spectrum recorded with **3** in hexanes containing 3 mM MeOH (Figure 7a) showed a prompt absorption centered at $\lambda_{max} = 370$ nm, which decayed on the microsecond time scale to afford similar long-lived oligomer absorptions to those observed in the absence of substrate; SnPh$_2$ itself could not be detected under these conditions. We assign the 370 nm species to the SnPh$_2$−MeOH Lewis acid−base complex (**19**; eq 13). The stannylene could be detected at lower concentrations of MeOH, where it was found to exhibit bimodal decays consisting of a rapid initial decay component and a slowly decaying residual absorbance. The initial decay became more rapid and the intensity of the residual absorbance was reduced as the MeOH concentration was increased, which is consistent with a reversible reaction characterized by an equilibrium constant in the approximate range of 2×10^3 M^{-1} < K_{MeOH} < 3×10^4 M^{-1}.[35] Analysis of the transient decay and residual signal intensity data in the usual manner[35] (see Figure 6b) afforded rate and equilibrium constants of $k_{MeOH} = (6 \pm 1) \times 10^9$ M^{-1} s^{-1} and $K_{MeOH} = (7.6 \pm 0.8) \times 10^3$ M^{-1}, respectively.

The 3-fold higher value of K_{MeOH} for SnPh$_2$ compared to SnMe$_2$ corresponds to a difference in binding free energies of ca. 0.7 kcal mol^{-1}, which is similar to that reported for complexation of MeOH with the corresponding Ge(II) homologues (GeMe$_2$, $K_{MeOH} = 900$ M^{-1}; GePh$_2$, $K_{MeOH} = 3300$ M^{-1}).[35b,37] The data indicate that with both the methyl-

and phenyl-substituted MR$_2$ (M = Si, Ge, or Sn) systems the Lewis acidity at the central M(II) atom is modestly higher for the stannylenes than the germylenes, the difference in binding free energies of the Sn(II) and Ge(II) complexes (all else being equal) amounting to about 0.5 kcal mol^{-1} for both substituents. The acidity-enhancing effect of phenyl substitution at the M(II) center is also observed with the corresponding silylenes, which (based on our earlier estimates of K_{MeOH}[35b]) are modestly stronger Lewis acids than the stannylenes. Thus, Lewis acidity decreases in the order SiR$_2$ > SnR$_2$ > GeR$_2$ for both substituents. Interestingly, the UV−vis spectra of the stannylene−MeOH complexes are both red-shifted significantly compared to those of the corresponding SiR$_2$−MeOH and GeR$_2$−MeOH complexes.[35a,37]

The absolute rate and equilibrium constants determined above for the dimerization of SnMe$_2$ and SnPh$_2$ and their reactions with Me$_2$SnCl$_2$ and MeOH in hexanes at 25 °C are summarized in Table 1.

Table 1. Absolute Rate (k, M^{-1} s^{-1}) and(or) Equilibrium Constants (K, M^{-1}) for Dimerization and Reactions of Dimethylstannylene (SnMe$_2$) and Diphenylstannylene (SnPh$_2$) with Me$_2$SnCl$_2$ and MeOH, Determined by Laser Flash Photolysis of 2 and 3 in Hexanes Solution at 25 °C[a]

|	k (M^{-1} s^{-1}) [K (M^{-1})]	
substrate	SnMe$_2$	SnPh$_2$
SnR$_2$ (dimerization)	$(1.4 \pm 0.4) \times 10^{10}$	$(1.6 \pm 0.4) \times 10^{10}$
Me$_2$SnCl$_2$	$(1.9 \pm 0.3) \times 10^{10}$	$(3.6 \pm 0.2) \times 10^9$
MeOH	$-[(2.4 \pm 0.2) \times 10^3]$	$(6 \pm 1) \times 10^9$
		$[(7.6 \pm 0.8) \times 10^3]$

[a]Equilibrium constants are denoted by square brackets.

Computational Studies. DFT calculations were carried out to model the structures, relative energies, and electronic spectra of SnMe$_2$, SnPh$_2$, the corresponding distannene and stannylstannylene dimers, and the Lewis acid−base complexes of the two SnR$_2$ species with MeOH and to attempt to identify a possible mechanism for the apparent diffusion-controlled formation of stannylstannylene **17b** from dimerization of

Table 2. Calculated Electronic Energies, Enthalpies (298.15 K), and Free Energies (298.15 K) of Stationary Points in the Dimerization of SnMe$_2$ and SnPh$_2$ and Their Lewis Acid−Base Complexation with Methanol, Calculated at the ωB97XD/6-31+G(d,p)^{C,H,O}-LANL2DZdp^{Sn} Level of Theory Relative to the Isolated Reactants (in kcal mol^{-1})^a

| | ωB97XD/6-31+G(d,p)^{C,H,O}-LANL2DZdp^{Sn} | | |
species	ΔE_{elec}	$\Delta H°$	$\Delta G°$
Me$_2$Sn=SnMe$_2$ (**16a**)	−24.9	−22.1	−11.9
MeSnSnMe$_3$ (**17a**)	−32.7	−30.3	−21.1
Ph$_2$Sn=SnPh$_2$ (**16b**)	−22.7	−21.1	−11.4
PhSnSnPh$_3$ (**17b**)^b	−34.0	−33.0	−21.1
PhSn(C$_6$H$_5$)SnPh$_2$ (**20**)	−29.8	−28.3	−16.3
trans-PhSn(C$_6$H$_5$)$_2$SnPh (**21**)	−19.5	−18.0	−5.8
transition state **25**‡	+0.4	+1.0	+14.4
transition state **26**^{‡c}	−29.2	−28.5	−15.7
Me$_2$Sn−O(H)Me (**18**)^d	−13.5 (−14.4)	−11.8 (−12.8)	−1.9 (−2.9)
Ph$_2$Sn−O(H)Me (**19**)^d	−16.0 (−17.3)	−14.3 (−15.6)	−3.3 (−5.0)

^{a}Thermodynamic parameters were computed at 298.15 K from unscaled vibrational frequencies. ^{b}Structure gives rise to one low-energy imaginary frequency (= 8.21i cm^{-1}). ^{c}An IRC calculation showed that **26**‡ is in fact not the correct transition state for the formation of **17b** from **20**. However, its calculated energies define upper limits for those of the true transition state for the process. ^{d}Corrected for BSSE; values in parentheses are the corresponding uncorrected values.

SnPh$_2$. The calculations employed the dispersion-corrected hybrid density functional of Chai and Head-Gordon (ωB97XD)[38] in conjunction with the 6-31+G(d,p) basis set for first- and second-row elements and the LANL2DZdp basis set and effective core potential for Sn.[39] Energy minima were identified by the absence of negative eigenvalues of the Hessian matrix, while transition-state structures (*vide infra*) were identified as such by the presence of a single negative eigenvalue. A total of four Sn$_2$Ph$_4$ isomers were located (*vide infra*): distannene **16b**, stannylstannylene **17b**, and the mono- and dibridged SnPh$_2$ dimers **20** and **21**, respectively. All four of these structures corresponded to energy minima except for **17b**, which gave rise to one imaginary frequency associated with a coupled rocking vibration of two of the phenyl groups. Despite many attempts, we were unsuccessful at locating a minimum-energy geometry for this structure with the ωB97XD density functional.[40] All energies are referenced relative to the isolated stannylenes (+ MeOH, where appropriate) at 298.15 K; those for the complexes with MeOH are corrected for basis set superposition errors (BSSE), which were computed using the counterpoise correction method.[41] Vibrational frequencies were not scaled. Table 2 lists the calculated (ωB97XD/6-31+G-(d,p)^{C,H,O}-LANL2DZdp^{Sn}) electronic energies and thermochemical parameters of the various structures that were located computationally, relative to the isolated reactants. The structures and selected geometrical parameters of the various SnPh$_2$ dimers studied are shown in Figure S13 and in the reaction coordinate diagram of Figure 8 (*vide infra*).
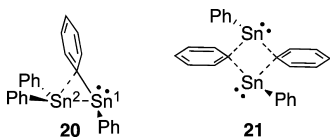
The stannylidenestannylene structure **20** is analogous to the "zwitterionic, donor−acceptor" stannylene dimers that have been reported by various groups,[9b,c,e,h,42] the bridging phenyl group in the present case providing π-stabilization of the increased positive charge at the neighboring Sn atom that results from the donor−acceptor interaction between the two Sn atoms. Indeed, NBO calculations afforded charges of +0.80 and +1.09 at the Sn^1 and Sn^2 atoms in **20**, respectively,

indicating discrete polarization of the Sn−Sn bond in the molecule.[43] The structure and bonding situation in both **20** and **21** are somewhat analogous to the sterically stabilized halogen- and hydride-bridged stannylene dimers (**22** and **23**, respectively) that have been reported by Power and co-workers.[9f,g] All of the possible SnPh$_2$-dimer isomers have precedent in the early theoretical studies of Trinquier of the dimers of SnH$_2$ and the other parent divalent group 14 hydrides.[29,44]
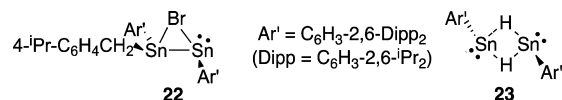
A parallel set of calculations was carried out using the ωB97X[45] density functional and the same basis set combination (see Table S1), to assess the effects of dispersion correction on the calculated energies.[46] For the stannylene dimers, the inclusion of dispersion corrections lowered the calculated energies by 1.5−6 kcal mol^{-1}, with the largest effects being on the bridged dimers **20** and **21**. As might be expected, it had little impact on the binding energies of the stannylene−MeOH complexes.

The calculated structures of SnMe$_2$, SnPh$_2$, and their doubly bonded dimers (**16a** and **16b**, respectively) compare favorably with previously reported structures at other levels of theory.[11b,12f,47] Similarly, the calculated Sn−Sn bond distances in the distannenes (2.74 and 2.77 Å for **16a** and **16b**, respectively) and the stannylstannylenes (2.91 and 2.90 Å for **17a** and **17b**, respectively) are in very good agreement with experimental data for the tetraalkyl- and tetraaryldistannene and stannylstannylene derivatives for which structural data exist.[2g,9a,d,f,48] As is the case with the parent hydrido systems,[29] the stannylstannylenes are in both cases predicted to be significantly lower in energy than the corresponding distannene isomer. The difference is larger for the phenylated systems, presumably reflecting a weakening effect of phenyl substitution on the Sn=Sn bond strength (see Table 2).[11b]

Excellent agreement is also observed between the calculated (BSSE-corrected, gas phase) free energies of complexation of MeOH with SnMe$_2$ ($\Delta G = -1.9$ kcal mol^{-1}) and SnPh$_2$ ($\Delta G = -3.3$ kcal mol^{-1}) and the experimental (solution phase) values of $\Delta G = -2.7$ and -3.3 kcal mol^{-1}, respectively, where the
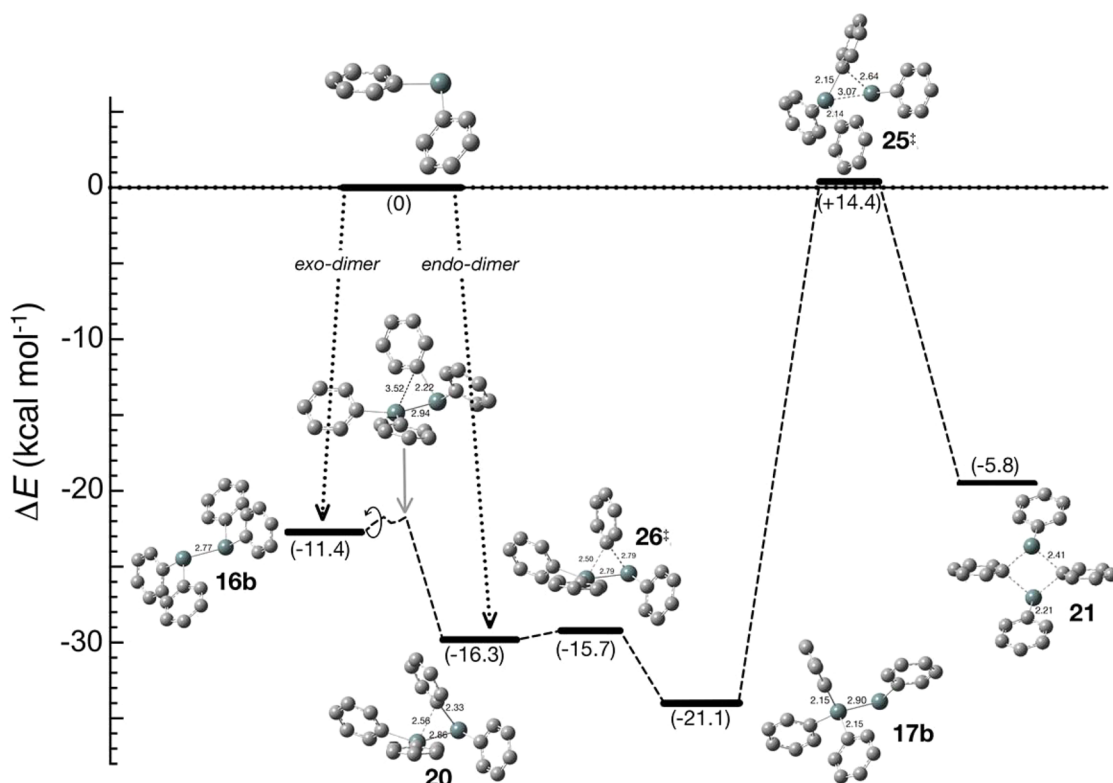
Figure 8. Electronic energy vs reaction coordinate diagram for the dimerization of $SnPh_2$ and interconversion of the $(SnPh_2)_2$ isomers, calculated at the $\omega B97XD/6\text{-}31\text{+}G(d,p)^{C,H,O}\text{-}LANL2DZdp^{Sn}$ level of theory. The vertical placement of the various structures is defined by their calculated electronic energy relative to (twice) that of $SnPh_2$ (1 atm gas phase, 0 K), as indicated on the y-axis; the numbers in parentheses are the corresponding standard free energies (see Table 2).

latter were calculated from the equilibrium constants after adjustment to the gas phase reference state (1 atm, 298.15 K). This gives some confidence in the chemical accuracy of the $\omega B97XD/6\text{-}31\text{+}G(d,p)^{C,H}\text{-}LANL2DZdp^{Sn}$ method for the prediction of reaction thermochemistries for transient Sn(II) systems, at least as applied to Lewis acid−base complexation reactions.

Electronic spectra were modeled using the time-dependent (TD) extension of the $\omega B97XD$ functional and the same basis set combination as was employed for the geometry optimizations; the results of the calculations are listed in Table 3 along with the corresponding experimental values where known. Again, reasonable agreement between theory and experiment is observed in all cases for which comparisons are possible; these include $SnMe_2$, $SnPh_2$, $Me_2Sn=SnMe_2$ (**16a**), and the two stannylene−MeOH complexes, for which the TDDFT predictions of the lowest energy electronic transitions agree with the experimental values to within 0.15 eV in every case. The calculated absorption maximum for $Ph_2Sn=SnPh_2$ (**16b**; $\lambda_{max} \approx 503$ nm) is within the range of reported values for kinetically stable tetraaryldistannenes[25a,27] and supports the conclusion that the $SnPh_2$ dimer detected by laser photolysis of **3** is *not* the distannene. As mentioned above, the most likely alternative based on thermodynamic considerations is stannylstannylene **17b**,[2g] for which the TDDFT calculation predicts a very weak HOMO → LUMO (n → 5p) absorption centered at $\lambda_{max} \approx 730$ nm, in reasonable agreement with the value reported for the stable derivative **24** ($\lambda_{max} \approx 689$ nm; $\varepsilon = 271$ M^{-1} cm^{-1})[9d] and consistent with the weak secondary product absorption at 650 nm observed by laser photolysis of **3** (*vide supra*). It should be noted that the calculated oscillator strength

Table 3. Calculated[a] and Experimental UV−Vis Absorption Maxima of Stannylenes and Stannylene-Derived Dimers and Methanol Complexes

	λ_{max}/nm (f)	
compound	calculated[a]	experimental
$SnMe_2$	515(0.029)	500
$SnPh_2$	331(0.143), 495(0.027)	290, 505
$Me_2Sn=SnMe_2$ (**16a**)	440(0.351)	465
$MeSnSnMe_3$ (**17a**)	270(0.095), 400(0.011), 800(0.002)	
$Ph_2Sn=SnPh_2$ (**16b**)	275(0.123), 503(0.353)	
$PhSnSnPh_3$ (**17b**)	288(0.149), 383(0.016), 730(0.001)	< 280, ~340(sh), 650[b]
$PhSn(C_6H_5)SnPh_2$ (**20**)	284(0.318), 337(0.013), 386(0.115)	
$PhSn(C_6H_5)_2SnPh$ (**21**)	279(0.070), 323(0.242), 338(0.186)	
$Me_2Sn-O(H)Me$ (**18**)	254(0.19), 348(0.08)	355
$Ph_2Sn-O(H)Me$ (**19**)	241(0.23), 354(0.05)	370

[a]TD-$\omega B97XD/6\text{-}31\text{+}G(d,p)^{C,H,O}\text{-}LANL2DZdp^{Sn}//\omega B97XD/6\text{-}31\text{+}G(d,p)^{C,H,O}\text{-}LANL2DZdp^{Sn}$; the numbers in parentheses are the calculated oscillator strengths (f) of each of the transitions. [b]The UV−vis spectrum of the experimentally observed $SnPh_2$ dimer consists of a broad absorption extending from 270 to 400 nm (Figures 5 and S10a). A very weak absorption at 650 nm, with similar growth/decay characteristics to those recorded at 340−360 nm, was also detected (Figure S10b) and is tentatively ascribed to the same species.

of the n → 5p transition in **17b** is an order of magnitude smaller than that calculated for the corresponding transition in SnPh$_2$ (see Table 3), which is also in good agreement with the difference between the experimental extinction coefficients of the stable stannylstannylene **24**[9d] and SnPh$_2$ (*vide supra*). The long-wavelength n → 5p absorption band in the spectrum of **17b** is thus expected to be inherently quite difficult to detect under the conditions of our laser photolysis experiments.

(Trip = 2,4,6-(*i*-Pr)$_3$C$_6$H$_2$)

24
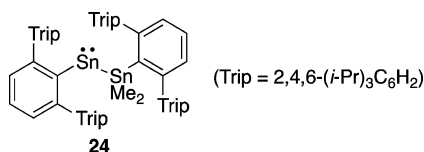
We next probed possible mechanisms for the formation of **17b** via rearrangement of distannene **16b**, which we assumed to be the first-formed product in the dimerization of SnPh$_2$. We began by modeling transition-state structure **25**‡, using a starting geometry derived from the structure reported by Tsai and Su[12g] in their computational study of the reversible dimerization/valence isomerization of a bulky arylphenylstannylene derivative reported in 2003 by Power and co-workers (eq 15).[2g] The structure that was located (**25**‡) indeed



(15)

(16)

17b   **25**‡ **21**
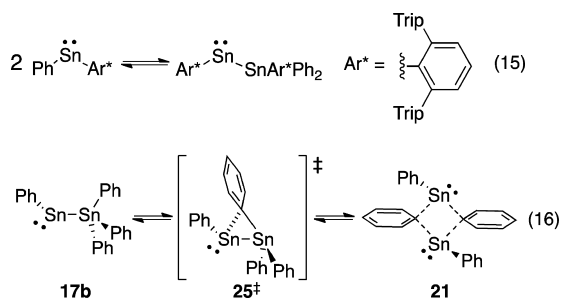
corresponds closely to that reported in the earlier study.[12g] However, it is much too high in energy to be compatible with the kinetic data, which indicate that the initial dimerization step is the rate-determining step in the sequence, and all subsequent unimolecular rearrangement steps must occur on the nanosecond (or shorter) time scale. Indeed, an intrinsic reaction coordinate (IRC) calculation showed that **25**‡ links stannylstannylene **17b** to the doubly bridged dimer **21** (eq 16) and not to distannene **16b**.

We then carried out a relaxed potential energy surface (PES) scan of the trans C$_{Ph}$–Sn–Sn–C$_{Ph}$ dihedral angles in **16b**, based on the hypothesis that the [1,2]-phenyl migration that leads to **17b** is likely to be preceded by twisting about the Sn═Sn bond, to allow the migrating Sn–C bond to adopt an orientation in which it roughly bisects the C–Sn–C angle at the second Sn atom. Interestingly, contracting either of the trans dihedral angles in 10° increments from the equilibrium geometry resulted in initial flattening of one end of the Sn═Sn bond and concomitant flipping of the substituents at the other end into a near-perpendicular relative orientation, as the dihedral was contracted through the initial 50–60° of the rotation. The process (see eq 17 and Figure S14A) resulted in less than a 2 kcal mol^{-1} rise in energy as the molecule approached the perpendicular orientation, after which continued rotation resulted in an abrupt drop in energy and the formation of the singly bridged dimer **20**. Structure **20** evidently occupies a rather shallow minimum on the Sn$_2$Ph$_4$ PES, as various attempts to locate an analogous structure at the

(17)

16b   **20**
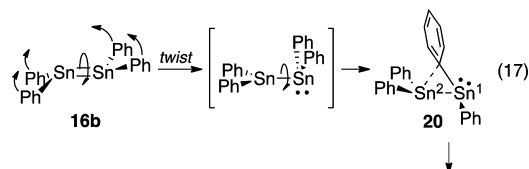
B3LYP/LANL2DZ level of theory all failed, most of them leading instead to the global minimum, stannylstannylene **17b**.

A relaxed PES scan of the bridging Sn–C bond distance in **20** was then carried out in an attempt to locate a transition state for migration of the bridging phenyl group to form **17b**. Decreasing the bridging Sn–C distance (bond "a" in eq 18) in

(18)

20   **26**‡ **17b**
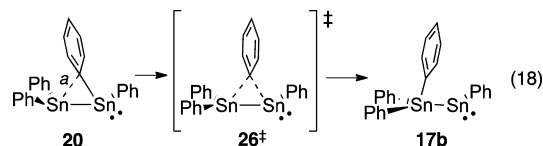
increments of 0.03 Å from its equilibrium value (of 2.56 Å) in **20** resulted in a rise in ΔE of only 0.5 kcal mol^{-1} at the highest energy point in the migration, which was successfully optimized to transition-state structure **26**‡ (see eq 18 and Figure S15). While an IRC calculation revealed that **26**‡ is in fact not the correct transition state linking **20** and **17b**, it nevertheless represents an upper energetic limit in the reaction profile for interconversion of the two isomers, which is shown in Figure S14B along with the computed structures at selected points in the transformation.

Finally, relaxed scan calculations of the Sn–Sn bond distances in **16b** and **20** were carried out in a search for potential transition states for their direct formation via SnPh$_2$ dimerization. Incremental lengthening of the Sn–Sn bond distances (d_{Sn-Sn}) in the two molecules to values in excess of 4 Å resulted simply in a continuous rise in energy in both cases (see Figure S15). The calculation for **16b** essentially collapsed once the Sn–Sn distance exceeded 4 Å, but with **20**, stabilizing nonbonded (π–π) interactions between the bridging phenyl group and the neighboring Sn atom persisted even at Sn–Sn distances as large as 6.5 Å.[12i] In neither case could any indication of a possible transition state be found. This suggests there are *two* distinct barrierless pathways for dimerization of SnPh$_2$, one involving exo approach of one stannylene toward the other and leading to distannene **16b**, and the other involving an endo approach and leading to the polarized stannylidenestannylene structure, **20**. With a predicted barrier of less than 1 kcal mol^{-1} for the phenyl migration that converts **20** to **17b**, the endo dimerization pathway comes very close to the limit of concerted insertion of one SnPh$_2$ unit into a Sn–C(Ph) bond of another, assisted by π$_{Ph}$→p$_{Sn}$ dative bonding interactions.

Thus, the calculations support a multistep mechanism for the formation of stannylstannylene **17b** via dimerization of SnPh$_2$, in which the initial diffusional encounter of the two stannylene moieties is the rate-determining step in the sequence. The two possible products of the initial step—distannene **16b** and stannylidenestannylene **20**—are each formed by barrierless pathways and represent shallow minima on the (SnPh$_2$)$_2$ energy surface, according to the calculations. Both species are predicted to have lifetimes in the nanosecond range or less, due to the ultrafast phenyl-migration process that leads from distannene **16b** to stannylstannylene **17b** via the intermediacy

of the phenyl-bridged isomer, **20**. The calculations, which are summarized in Figure 8 in the form of a reaction coordinate diagram for interconversion of the various $(SnPh_2)_2$ dimer structures, are fully consistent with the experimental kinetic data.

■ SUMMARY AND CONCLUSIONS

The transient stannylenes $SnMe_2$ and $SnPh_2$ are formed cleanly and efficiently by UV-lamp or -laser photolysis of the 1-stannacyclopent-3-ene derivatives **2** and **3**, respectively, according to the results of chemical trapping and laser flash photolysis experiments. The stannylenes can both be trapped cleanly by Sn−Cl insertion with Me_2SnCl_2 in aerated solution, the presence of air facilitating the reaction by oxidizing the initially produced 1,2-dichlorostannanes, which absorb relatively strongly at the excitation wavelength and are themselves highly photolabile; the corresponding 1,3-dichlorodistannoxanes that are formed in the oxidation absorb relatively weakly at the photolysis wavelength and exhibit very low photoreactivity. The ultimate product of trapping *both* $SnMe_2$ and $SnPh_2$ with Me_2SnCl_2 under these conditions is the association dimer of 1,3-dichlorotetramethyldistannoxane (**6**), along with Ph_2SnCl_2 (**8**) in the case of $SnPh_2$. In the latter case, dichlorostannane **8** is liberated from the initially formed dichlorodistannoxane dimer (**11**) by exchange with excess Me_2SnCl_2; this process has been verified to be rapid and reversible under conditions similar to those employed in our photolysis experiments. The two-step exchange reaction is characterized by equilibrium constants that indicate that phenyl substitution on the peripheral Sn atoms leads to increased stabilization of the dimer compared to methyl substitution.

Both transient stannylenes are detectable by laser flash photolysis, their long-wavelength (n → 5p) absorption bands centered at λ_{max} = 500 nm ($SnMe_2$; ε_{500} = 1800 ± 600 M^{-1} cm^{-1}) and λ_{max} = 505 nm ($SnPh_2$; ε_{500} = 2400 ± 600 M^{-1} cm^{-1}). They each decay with a second-order rate constant approaching the diffusional limit, with the concomitant growth of secondary transient absorptions assignable to the corresponding dimers. Both stannylenes react rapidly with added Me_2SnCl_2, $SnMe_2$ with an absolute rate constant of k_Q = (1.9 ± 0.3) × 10^{10} and $SnPh_2$ with k_Q = (3.6 ± 0.2) × 10^9 M^{-1} s^{-1} in hexanes at 25 °C.

The UV−vis spectrum and dimerization behavior of $SnMe_2$ agrees well with earlier solution phase results,[11b] the species decaying with clean second-order kinetics (k_{dim} = (1.4 ± 0.4) × 10^{10} M^{-1} s^{-1}) to afford tetramethyldistannene ($Me_2Sn=SnMe_2$, **16a**; λ_{max} = 465 nm). The distannene absorption decays on a similar time scale as those due to $SnMe_2$, to afford one or more longer lived product(s) exhibiting absorptions below 360 nm. Diphenylstannylene also dimerizes at close to the diffusion-controlled rate (k_{dim} = (1.6 ± 0.4) × 10^{10} M^{-1} s^{-1}), but in contrast to the behavior exhibited by the dialkyl derivative, the UV−vis spectrum of the observed $SnPh_2$ dimer lacks the strong absorption in the 450−600 nm range that is expected for tetraphenyldistannene ($Ph_2Sn=SnPh_2$, **16b**). The observed dimer (λ_{max} = 280, 340(sh) nm) is instead assigned to phenyltriphenylstannylstannylene (**17b**), based on the observation of a weak transient product absorption centered at 650 nm, which is in the range expected for such a species, and the results of DFT calculations carried out at the ωB97XD/6-31+G(d,p)^{C,H,O}-LANL2DZdp^{Sn} level of theory. The latter indicate that **17b** is the global minimum on the Sn_2Ph_4 potential energy surface and suggest it can be formed from the higher energy distannene isomer via an ultrafast rearrangement process involving the intermediacy of a phenyl-bridged donor−acceptor dimer (**20**). The calculated reaction barriers are consistent with the experimental finding that diffusion is the rate-controlling step in the decay of $SnPh_2$ and the formation of **17b** in hexanes at 25 °C. The calculations further suggest that the phenyl-bridged dimer can also be formed via a direct endo dimerization pathway, which should compete with the exo pathway that produces the isomeric distannene. According to the calculations, the barrier for migration of the bridging phenyl group in **20** is so low that the endo dimerization mode represents an essentially *direct* (formal Sn−C(Ph) insertion) pathway for the formation of **17b** from $SnPh_2$.

Further exploration of the kinetics and thermodynamics of the reactions of transient stannylene derivatives in solution is in progress.

■ EXPERIMENTAL SECTION

^1H, ^{13}C, and ^{119}Sn NMR spectra were recorded at 600.13 MHz (^1H), 150.90 MHz ($^{13}C\{^1H\}$), and 223.79 MHz ($^{119}Sn\{^1H\}$), respectively, on a Bruker AV600 spectrometer in deuterated chloroform, benzene-d_6, or cyclohexane-d_{12}. ^1H and ^{13}C NMR spectra were referenced to the residual solvent proton and ^{13}C signals, respectively, while ^{119}Sn spectra were recorded using the inverse-gated ^1H-decoupling scheme with a 30-degree pulse on ^{119}Sn and were referenced to an external solution of tetramethylstannane. High-resolution electron impact mass spectra and exact masses were determined on a Micromass TofSpec 2E mass spectrometer using electron impact ionization (70 eV). Infrared spectra were recorded as thin films on sodium chloride plates using a Nicolet 6700 FTIR spectrometer. Melting points were measured using a Mettler FP82 hot stage mounted on an Olympus BH-2 microscope and controlled by a Mettler FP80 central processor. Column chromatography was carried out using SiliaFlash P60 40−63 μm (230−400 mesh) silica gel (Silicycle).

All commercially available materials were used as received from the suppliers unless otherwise noted; solvents were all reagent grade or better. Tetrahydrofuran (THF) was distilled under nitrogen from sodium/benzophenone. Hexanes (HPLC grade) and diethyl ether were dried by passage through activated alumina under nitrogen using a Solv-Tek solvent purification system (Solv-Tek, Inc.). Naphthalene was purified by sublimation, while 2,3-dimethyl-1,3-butadiene (DMB; 98%) and 1,2-dibromoethane (98%) were purified by passage through a silica microcolumn immediately prior to use. Dichlorodimethyl-stannane used in steady state and laser photolysis experiments was purified by sublimation immediately prior to use. Methanol was distilled from sodium methoxide.

2-Methyl-3-phenyl-1,3-butadiene (**4a**) was prepared from 1-phenyl-1,2-propanedione by the method of Alder and co-workers[49] and purified by column chromatography (silica gel, hexanes). The compound was obtained as a colorless liquid exhibiting ^1H and ^{13}C NMR spectra that were in good agreement with reported data.[13] The 1-stannacyclopent-3-enes **2** and **3** were prepared according to procedures adapted from those of Gaspar and co-workers,[7] with the requisite magnesacycles being prepared according to the methods of Rieke and Xiong.[50]

Synthesis of 1,1,3-Trimethyl-4-phenyl-1-stannacyclopent-3-ene (2). To a solution of anhydrous $MgBr_2$, prepared *in situ* by addition of 1,2-dibromoethane (5.00 mL, 10.85 g, 0.058 mol) to Mg turnings (1.34 g, 0.055 g-atom) in THF (80 mL), were added freshly cut lithium wire (0.78 g, 0.113 g-atom) and naphthalene (2.19 g, 0.0171 mol). The mixture was stirred vigorously at room temperature for 18 h, at which point the lithium was fully consumed. The finely divided activated magnesium (Mg*) was allowed to settle, and the supernatant was removed by syringe and replaced with fresh THF (ca. 135 mL). The washing step was repeated, and then **4a** (7.63 g, 0.053 mol) was added as the neat liquid in a single portion. The resulting orange-brown solution was stirred for an additional 8 h, and the residual solids were allowed to settle.

A flame-dried 500 mL two-neck round-bottom flask equipped with a stir bar, septum, and addition funnel was charged with Me_2SnCl_2 (3.29 g, 0.015 mol) and dry THF (250 mL) under an atmosphere of argon and then cooled to −78 °C in an acetone/dry ice bath. The solution of (2-methyl-3-phenyl-2-butene-1,4-diyl)magnesium in THF prepared above was transferred to the flask dropwise until the reaction mixture tested neutral on moist pH paper (ca. 3 h). An additional portion of Me_2SnCl_2 (2.74 g, 0.012 mol) was added, and dropwise addition of the organomagnesium reagent was resumed until the pH again tested neutral (ca. 2 h). The reaction mixture was stirred and allowed to warm to room temperature overnight, and then transferred to a separatory funnel and washed with saturated aqueous ammonium chloride (3 × 75 mL). The combined aqueous extracts were extracted with diethyl ether (3 × 40 mL). The organic fractions were combined, dried over $MgSO_4$, and filtered, and the solvent was removed to yield a yellow, viscous liquid (12.53 g), which was estimated to consist of **2**, naphthalene, and **4a** in a ratio of 1:0.09:0.09 (estimated crude yield of **2** = 120%).

Isolation and purification of **2** from the crude reaction mixture was carried out as follows. Pentane (ca. 25 mL) was added to the oil from above, resulting in the formation of a white precipitate. The supernatant was decanted, and the solvent was removed on a rotary evaporator. The residue was then distilled (60 °C, 0.03 Torr) using a Kugelrohr distillation apparatus, collecting 2.23 g of a pale yellow oil. This procedure was repeated twice more with the viscous residue that remained after distillation, affording pale yellow oils with masses of 0.81 and 0.57 g. The ^{1}H NMR spectra of the three collected fractions showed them to consist of a mixture of **2**, naphthalene, and **4a** in relative ratios of 1.0:0.12:0.27, 1.0:0.02:0.19, and 1.0:0:0.10, respectively. The first fraction was pumped under high vacuum for ca. 9 h to obtain a mixture (1.72 g) of **2**, naphthalene, and **4a** in a ratio of 1:0.03:0.08. The second fraction was further purified by column chromatography (silica gel; hexanes/dichloromethane gradient (100:0 to 70:30)), the fractions containing **2** were collected, and solvent was removed to obtain a clear colorless oil (0.50 g) containing a mixture of **2** and **4a** in a molar ratio of 1:0.06. The latter two fractions were then combined and distilled (60 °C, 0.03 Torr) to afford a clear colorless oil (0.93 g) in which only **4a** could be detected as an impurity. This was then pumped under high vacuum (0.02 Torr) at room temperature for ca. 18 h to afford **2** as a colorless oil (0.59 g, 0.002 mol, 7.3%). The purity was estimated to be ≥98% by ^{1}H NMR spectroscopy, the major detectable contaminant being **4a**. ^{1}H NMR ($CDCl_3$): δ 0.34 (s, 6H, $^2J_{SnH}$ = 54.0, 56.1 Hz, Me_2Sn), 1.71 (m, 3H, $(-CH_2C(Me)C(Ph)-CH_2-)$), 1.76 (m, 2H, $^2J_{SnH}$ = 36.4 Hz, $(-CH_2C(Me)C(Ph)CH_2-)$), 1.92 (m, 2H, ^5J = 1.8 Hz, $^2J_{SnH}$ = 37.6 Hz, $(-CH_2C(Me)C(Ph)-CH_2-)$), 7.17 (d, 2H, ^3J = 6.9 Hz, o-Ph), 7.19 (t, 1H, ^3J = 7.3 Hz, p-Ph), 7.30 (t, 2H, ^3J = 7.6 Hz, m-Ph). ^{13}C{^{1}H} NMR ($CDCl_3$): δ −9.91 ($^1J_{SnC}$ = 309.8, 324.3 Hz, $(Me_2$Sn$)$), 21.91 ($^1J_{SnC}$ = 306.2, 320.8 Hz, $(-CH_2C(Me)C(Ph)CH_2-)$), 22.37 ($^1J_{SnC}$ = 297.6, 311.7 Hz ($-CH_2C(Me)C(Ph)CH_2-)$), 22.97 ($^3J_{SnC}$ = 59.9 Hz, $(-CH_2C(Me)C(Ph)CH_2-)$), 125.48 (p-Ph), 127.85 (m-Ph), 128.06 (o-Ph), 135.73 ($^2J_{SnC}$ = 17.1 Hz, $(-CH_2C(Me)C(Ph)CH_2-)$), 137.89 ($^2J_{SnC}$ = 20.4 Hz, $(-CH_2C(Me)C(Ph)CH_2-)$), 146.16 ($^3J_{SnC}$ = 55.3 Hz, (ipso-Ph)). ^{119}Sn{^{1}H} NMR ($CDCl_3$): δ 34.0. IR, cm^{-1} (relative intensity): 2976 (w), 2906 (m), 1491 (w), 1439 (w), 1103 (w), 890 (w), 766 (w), 700 (m). EI-MS, m/z (relative intensity; Sn-containing isotopomeric clusters are represented by the ^{120}Sn isotopomer and are indicated with an asterisk): 294.0* (26, M$^+$), 279.0* (78, M$^+$ − CH$_3$), 144.1 (22, M$^+$ − C$_2$H$_6$Sn), 134.9* (100, MeSn$^+$), 129.1 (52, C$_{10}$H$_9^+$), 128.1 (37, C$_{10}$H$_8^+$), 119.9* (14, Sn$^+$), 115.1 (15, C$_9$H$_7^+$), 77.0 (11, C$_6$H$_5^+$). HRMS: C$_{18}$H$_{20}^{120}$Sn calcd 294.0430, found 294.0447. The actual ^{1}H and ^{13}C NMR spectra of compound **2** are shown in Figure S16.

3,4-Dimethyl-1,1-diphenyl-1-stannacyclopent-3-ene (3).[7] A THF solution of lithium naphthalenide (prepared by stirring naphthalene (16.94 g, 0.132 mol) with lithium wire (0.84 g, 0.121 g-atom) in 75 mL of THF for 8 h) was added dropwise with rapid stirring to a solution of anhydrous magnesium bromide, generated by reaction of 1,2-dibromoethane (5.0 mL, 0.058 mol) with Mg turnings (1.34 g, 0.055 g-atom) in THF (80 mL). The resulting dark gray slurry of Mg* was allowed to settle, and the supernatant was removed and

replaced with fresh THF (135 mL). The washing step was repeated, and then 2,3-dimethyl-1,3-butadiene (6.2 mL, 0.055 mol) was added in one portion. The mixture was stirred for an additional 8 h, the precipitate was allowed to settle, and the resulting orange solution of (2,3-dimethyl-2-butene-1,4-diyl)magnesium in THF was removed by syringe and used directly in the following step.

A 500 mL flame-dried two-neck round-bottom flask equipped with a stir bar, septum, and addition funnel was charged with Ph_2SnCl_2 (4.81 g, 0.0140 mol) and THF (250 mL), and the resulting solution was cooled to −78 °C in an acetone/dry ice bath. The solution of (2,3-dimethyl-2-butene-1,4-diyl)magnesium in THF prepared above was then added dropwise over 8 h. The reaction mixture was monitored periodically using moist pH paper, and addition was stopped when the solution reached neutrality. The mixture was stirred while the bath warmed to room temperature overnight, after which it was washed with saturated aqueous NH$_4$Cl (3 × 75 mL), and the combined aqueous extracts were back-extracted with diethyl ether (3 × 40 mL). The combined organic extracts were dried over anhydrous MgSO$_4$ and the solvent was removed to afford a pale yellow oil, to which pentane (ca. 30 mL) was added to precipitate salts. The supernatant was decanted, and the solvent removed to yield a pale yellow oil (1.87 g). Further purification by column chromatography (silica gel; hexanes/dichloromethane gradient (100:0 to 70:30)) afforded a white solid (1.32 g, 3.72 mmol, 27%). Repeated recrystallization from methanol afforded colorless crystals that were identified as **3** (mp 45.9−46.8 °C) on the basis of their ^{1}H, ^{13}C{^{1}H}, and ^{119}Sn{^{1}H} NMR, IR, and mass spectra (Sn isotopomeric clusters are represented by the ^{120}Sn isotopomer and are indicated with an asterisk). ^{1}H NMR (C$_6$D$_6$): δ 1.82 (s, 6H, CMe), 1.92 (s, 4H, $^2J_{SnH}$ = 39.3 Hz, $-CH_2C(Me)C(Me)CH_2-$), 7.18 (m, 6H, (o,p-Ph)), 7.51 (m, 4H, $^4J_{SnH}$ = 48.4 Hz, (m-Ph)). ^{13}C{^{1}H} NMR (C$_6$D$_6$): δ 21.46 ($-CH_2C(Me)C(Me)CH_2-$), 21.65 ($-CH_2C(Me)C(Me)CH_2-$), 128.68 ($^2J_{SnC}$ = 49.1 Hz, (o-Ph)), 128.98 ($^4J_{SnC}$ = 11.1 Hz, (p-Ph)), 131.68 ($-CH_2C(Me)C(Me)CH_2-$), 137.09 ($^3J_{SnC}$ = 37.8 Hz, (m-Ph)), 138.69 (ipso-Ph). ^{119}Sn{^{1}H} NMR (C$_6$D$_6$): δ −34.2. IR, cm^{-1} (relative intensity): 3063 (w), 2909 (m), 1480 (w), 1428 (m), 1146 (w), 1075 (w), 997 (w), 727 (m), 698 (m). EI-MS, m/z (relative intensity): 356.1* (4, M$^+$), 274.0* (41, M$^+$ − C$_6$H$_{10}$), 196.9* (62, PhSn$^+$), 144.9 (5), 119.9* (100, Sn$^+$). HRMS: C$_{18}$H$_{20}^{120}$Sn calcd 356.0587, found 356.0579. Except for a few differences in the ^{13}C spectrum, the data are in good agreement with the reported data of Gaspar and co-workers.[7]

1,1-Dichloro-1,1,3,3-tetramethyldistannoxane dimer (6). This was synthesized by the method of Okawara and Wada[51] and obtained as a colorless, high-melting granular powder (mp >280 °C).[17c] The ^{1}H, ^{13}C, and ^{119}Sn NMR spectra of the compound in CDCl$_3$ and C$_6$D$_{12}$ are listed below; the spectra were recorded in the presence of ca. 40 and 25 mM Me$_2$SnCl$_2$, respectively, to facilitate dissolution. ^{1}H NMR (CDCl$_3$ + 40 mM Me$_2$SnCl$_2$): δ 1.18 (s, 12H, $^2J_{SnH}$ = 76.3, 79.5 Hz, (Me$_2$SnO)$_2$(Me$_2$SnCl$_2$)$_2$), 1.25 (s, 12H, $^2J_{SnH}$ = 81.4, 83.9 Hz, (Me$_2$SnO)$_2$(Me$_2$SnCl$_2$)$_2$). ^{1}H NMR (C$_6$D$_{12}$): δ 1.04 (s, 12H, $^2J_{SnH}$ = 76.8, 80.2 Hz, (Me$_2$SnO)$_2$(Me$_2$SnCl$_2$)$_2$), 1.15 (s, 12H, $^2J_{SnH}$ = 82.6, 85.4 Hz, (Me$_2$SnO)$_2$(Me$_2$SnCl$_2$)$_2$). ^{13}C{^{1}H} NMR (CDCl$_3$): δ 12.4 (Me$_2$SnO)$_2$(Me$_2$SnCl$_2$)$_2$), 13.7 (Me$_2$SnO)$_2$(Me$_2$SnCl$_2$)$_2$). ^{119}Sn{^{1}H} NMR (CDCl$_3$): δ −61.1 ($^2J_{SnSn}$ = 55.2 Hz (approx), (Me$_2$SnO)$_2$(Me$_2$SnCl$_2$)$_2$), −116.1 ($^2J_{SnSn}$ = 57.2 Hz, (Me$_2$SnO)$_2$(Me$_2$SnCl$_2$)$_2$). ^{119}Sn{^{1}H} NMR (C$_6$D$_{12}$): δ −63.2 (Me$_2$SnO)$_2$(Me$_2$SnCl$_2$)$_2$), −125.4 (Me$_2$SnO)$_2$(Me$_2$SnCl$_2$)$_2$). The ^{1}H and ^{119}Sn NMR spectra are in reasonable agreement with previously reported spectra.[17]

Dodecaphenylcyclohexastannane (c-Sn$_6$Ph$_{12}$). This was prepared according to the method of Neumann and König.[5e] The compound was obtained as colorless crystals (mp >270 °C (dec)[5e]), which exhibited ^{1}H and ^{119}Sn NMR spectra that are in reasonable agreement with published data for the compound.[52] ^{1}H NMR (CDCl$_3$): δ 7.02 (t, 24H, ^3J = 7.5 Hz, m-Ph), 7.20 (t, 12H, ^3J = 7.5 Hz, p-Ph), 7.25 (d, 24H, ^3J = 7.7 Hz, $^3J_{SnH}$ = 47.7 Hz, o-Ph). ^{13}C{^{1}H} NMR (CDCl$_3$): δ 128.23 ($^4J_{SnC}$ = 11.1 Hz, p-Ph), 128.55 ($^3J_{SnC}$ = 44.8 Hz, m-Ph), 138.26 ($^2J_{SnC}$ = 41.7 Hz, $^3J_{SnC}$ = 10.2 Hz, o-Ph), 138.62 ($^1J_{SnC}$ = 283.7 Hz, $^2J_{SnC}$ = 19.6 Hz, ipso-Ph). ^{119}Sn{^{1}H} NMR (CDCl$_3$): δ −207.5 ($^1J_{SnSn}$ = 1079.0 Hz, $^2J_{SnSn}$ = 779.9 Hz, c-Sn$_6$Ph$_{12}$).

Steady-state photolysis experiments were carried out using a Rayonet photochemical reactor (Southern New England Ultraviolet Co.) equipped with two RPR-2537 lamps as excitation source. Samples were contained in quartz NMR tubes mounted in a merry-go-round apparatus and were monitored at selected time intervals by ^{1}H NMR spectroscopy. Cyclohexane-d_{12} solutions containing the desired combinations of stannylene precursor, substrate, and hexamethyldisilane (ca. 0.01 M; internal integration standard) were prepared in 1 mL volumetric flasks. The solutions were transferred to the quartz NMR tubes, which were then sealed with rubber septa and deoxygenated with a slow stream of dry argon for 25 min prior to irradiation over a total time period of 5−10 min; "nondeaerated" solutions were simply used as prepared, For the quantum yield experiments, a slow stream of air was bubbled through the solutions both before irradiation commenced and in between each photolysis interval in order to maintain air saturation.

Laser flash photolysis experiments were carried out using a Lambda Physik Compex 120 excimer laser filled with F_2/Kr/Ne (248 nm, 20 ns, 99 ± 5 mJ) and a Luzchem Research mLFP-111 laser flash photolysis system, modified as described previously;[15] most experiments were carried out with the laser power reduced from the nominal value using neutral density filters (constructed from wire screening). The solutions were prepared in deoxygenated anhydrous hexanes such that the absorbance at 248 nm was between 0.4 and 0.7. The solutions were flowed through a 7 × 7 mm Suprasil flow cell from calibrated 100 or 250 mL reservoirs, which contain a glass frit to allow bubbling of argon gas through the solution for 40 min prior to and throughout the experiment. The flow cell was connected to a Masterflex 77390 peristaltic pump fitted with Teflon tubing (Cole-Parmer Instrument Co.), which pulls the solution through the cell at a constant rate of 2−3 mL/min. The glassware, sample cell, and transfer lines were dried in a vacuum oven (65−85 °C) before use. Solution temperatures were measured with a Teflon-coated copper/constantan thermocouple inserted into the thermostated sample compartment in close proximity to the sample cell. Substrates were added directly to the reservoir by microliter syringe as aliquots of standard solutions.

Transient absorbance−time profiles were recorded by signal averaging of data obtained from 10 to 40 individual laser shots. Decay rate constants were calculated by nonlinear least-squares analysis of the transient absorbance−time profiles using the Prism 5.0 software package (GraphPad Software, Inc.) and the appropriate user-defined fitting equations, after importing the raw data from the Luzchem mLFP software. Rate and equilibrium constants were calculated by linear least-squares analysis of transient absorbance data that spanned as large a range in transient decay rate or initial signal intensity as possible. Errors are quoted as twice the standard error obtained from the least-squares analyses.

Details of the theoretical calculations are given in the Supporting Information.

ASSOCIATED CONTENT

Ⓢ Supporting Information

The Supporting Information is available free of charge on the ACS Publications website at DOI: 10.1021/acs.organomet.5b00615.

> Representative NMR spectra and concentration vs time plots from steady-state photolysis experiments; determination of equilibrium constants for interconversion of **6**, **11**, and **12**; time-resolved UV−vis spectra and equilibrium constant data for the complexation of SnMe$_2$ with MeOH; details of the computational studies, including tables of geometrical data for the computed structures and details of relaxed PES scan calculations (PDF)

■ AUTHOR INFORMATION

Corresponding Author
*E-mail: leigh@mcmaster.ca.

Notes
The authors declare no competing financial interest.

■ ACKNOWLEDGMENTS

■ REFERENCES

(1) (a) Davidson, P. J.; Lappert, M. F. *J. Chem. Soc., Chem. Commun.* **1973**, 317a. (b) Cotton, J. D.; Davidson, P. J.; Lappert, M. F. *J. Chem. Soc., Dalton Trans.* **1976**, 2275. (c) Davidson, P. J.; Harris, D. H.; Lappert, M. F. *J. Chem. Soc., Dalton Trans.* **1976**, 2268. (d) Schager, F.; Goddard, R.; Seevogel, K.; Porschke, K. R. *Organometallics* **1998**, *17*, 1546. (e) Hillner, K.; Neumann, W. P. *Tetrahedron Lett.* **1986**, *27*, 5347. (f) Kira, M.; Yauchibara, R.; Hirano, R.; Kabuto, C.; Sakurai, H. *J. Am. Chem. Soc.* **1991**, *113*, 7785. (g) Eaborn, C.; Hill, M. S.; Hitchcock, P. B.; Patel, D.; Smith, J. D.; Zhang, S. *Organometallics* **2000**, *19*, 49. (h) Kavara, A.; Cousineau, K. D.; Rohr, A. D.; Kampf, J. W.; Banaszak Holl, M. M. *Organometallics* **2008**, *27*, 1041. (i) Kavara, A.; Boron, T. T.; Ahsan, Z. S.; Banaszak Holl, M. M. *Organometallics* **2010**, *29*, 5033.

(2) (a) Tokitoh, N.; Saito, M.; Okazaki, R. *J. Am. Chem. Soc.* **1993**, *115*, 2065. (b) Weidenbruch, M.; Schlaefke, J.; Schafer, A.; Peters, K.; von Schnering, H. G.; Marsmann, H. *Angew. Chem., Int. Ed. Engl.* **1994**, *33*, 1846. (c) Saito, M.; Tokitoh, N.; Okazaki, R. *Organometallics* **1996**, *15*, 4531. (d) Saito, M.; Tokitoh, N.; Okazaki, R. *Chem. Lett.* **1996**, *1996*, 265. (e) Saito, M.; Tokitoh, N.; Okazaki, R. *J. Am. Chem. Soc.* **1997**, *119*, 11124. (f) Simons, R. S.; Pu, L.; Olmstead, M. M.; Power, P. P. *Organometallics* **1997**, *16*, 1920. (g) Phillips, A. D.; Hino, S.; Power, P. P. *J. Am. Chem. Soc.* **2003**, *125*, 7520. (h) Spikes, G. H.; Peng, Y.; Fettinger, J. C.; Power, P. P. *Z. Anorg. Allg. Chem.* **2006**, *632*, 1005. (i) Tajima, T.; Takeda, N.; Sasamori, T.; Tokitoh, N. *Organometallics* **2006**, *25*, 3552. (j) Peng, Y.; Ellis, B. D.; Wang, X.; Power, P. P. *J. Am. Chem. Soc.* **2008**, *130*, 12268. (k) Peng, Y.; Guo, J.-D.; Ellis, B. D.; Zhu, Z.; Fettinger, J. C.; Nagase, S.; Power, P. P. *J. Am. Chem. Soc.* **2009**, *131*, 16272. (l) Dube, J. W.; Brown, Z. D.; Caputo, C. A.; Power, P. P.; Ragogna, P. J. *Chem. Commun.* **2014**, *50*, 1944. (m) Lips, F.; Mansikkamäki, A.; Fettinger, J. C.; Tuononen, H. M.; Power, P. P. *Organometallics* **2014**, *33*, 6253 10.1021/om500947x (n) Krebs, K. M.; Wiederkehr, J.; Schneider, J.; Schubert, H.; Eichele, K.; Wesemann, L. *Angew. Chem., Int. Ed.* **2015**, *54*, 5502.

(3) (a) Padelkova, Z.; Nechaev, M. S.; Lycka, A.; Holubova, J.; Zevaco, T. A.; Ruzicka, A. *Eur. J. Inorg. Chem.* **2009**, *2009*, 2058. (b) Padelkova, Z.; Vankatova, H.; Cisarova, I.; Nechaev, M. S.; Zevaco, T. A.; Walter, O.; Ruzicka, A. *Organometallics* **2009**, *28*, 2629. (c) Padelkova, Z.; Svec, P.; Pejchal, V.; Ruzicka, A. *Dalton Trans.* **2013**, *42*, 7660. (d) Freitag, S.; Henning, J.; Schubert, H.; Wesemann, L. *Angew. Chem., Int. Ed.* **2013**, *52*, 5640. (e) Freitag, S.; Krebs, K. M.; Henning, J.; Hirdler, J.; Schubert, H.; Wesemann, L. *Organometallics* **2013**, *32*, 6785. (f) Krebs, K. M.; Freitag, S.; Schubert, H.; Gerke, B.; Pöttgen, R.; Wesemann, L. *Chem. - Eur. J.* **2015**, *21*, 4628. (g) Sindlinger, C. P.; Wesemann, L. *Chem. Sci.* **2014**, *5*, 2739. (h) Sindlinger, C. P.; Weiß, S.; Schubert, H.; Wesemann, L. *Angew. Chem., Int. Ed.* **2015**, *54*, 4087.

(4) (a) Al-Rafia, S. M. I.; Malcolm, A. C.; Liew, S. K.; Ferguson, M. J.; Rivard, E. *J. Am. Chem. Soc.* **2011**, *133*, 777. (b) Al-Rafia, S. M. I.; Shynkaruk, O.; McDonald, S. M.; Liew, S. K.; Ferguson, M. J.;

McDonald, R.; Herber, R. H.; Rivard, E. *Inorg. Chem.* **2013**, *52*, 5581. (c) Rivard, E. *Dalton Trans.* **2014**, *43*, 8577. (d) Swarnakar, A. K.; McDonald, S. M.; Deutsch, K. C.; Choi, P.; Ferguson, M. J.; McDonald, R.; Rivard, E. *Inorg. Chem.* **2014**, *53*, 8662.

(5) (a) Krause, E.; Becker, R. *Ber. Dtsch. Chem. Ges. B* **1920**, *53*, 173. (b) Kuivila, H. G.; Jakusik, E. R. *J. Org. Chem.* **1961**, *26*, 1430. (c) Neumann, W. P.; König, K. *Angew. Chem., Int. Ed. Engl.* **1962**, *1*, 212. (d) Olson, D. H.; Rundle, R. E. *Inorg. Chem.* **1963**, *2*, 1310. (e) Neumann, W. P.; König, K. *J. Liebigs Ann. Chem.* **1964**, *677*, 1.

(6) (a) Neumann, W. P.; Schwarz, A. *Angew. Chem., Int. Ed. Engl.* **1975**, *14*, 812. (b) Schröer, U.; Neumann, W. P. *Angew. Chem., Int. Ed. Engl.* **1975**, *14*, 246. (c) Grugel, C.; Neumann, W. P.; Seifert, P. *Tetrahedron Lett.* **1977**, *18*, 2205. (d) Grugel, C.; Neumann, W. P.; Schriewer, M. *Angew. Chem., Int. Ed. Engl.* **1979**, *18*, 543. (e) Gross, L. W.; Moser, R.; Neumann, W. P.; Scherping, K. H. *Tetrahedron Lett.* **1982**, *23*, 635. (f) Scherping, K. H.; Neumann, W. P. *Organometallics* **1982**, *1*, 1017. (g) Watta, B.; Neumann, W. P.; Sauer, J. *Organometallics* **1985**, *4*, 1954. (h) Neumann, W. P. *Chem. Rev.* **1991**, *91*, 311.

(7) Zhou, D.; Reiche, C.; Nag, M.; Soderquist, J. A.; Gaspar, P. P. *Organometallics* **2009**, *28*, 2595.

(8) (a) Weidenbruch, M.; Schäfer, A.; Kilian, H.; Pohl, S.; Saak, W.; Marsmann, H. *Chem. Ber.* **1992**, *125*, 563. (b) Setaka, W.; Sakamoto, K.; Kira, M.; Power, P. P. *Organometallics* **2001**, *20*, 4460. (c) Kira, M.; Ishida, S.; Iwamoto, T. *Chem. Rec.* **2004**, *4*, 243. (d) Nag, M.; Gaspar, P. P. *Organometallics* **2009**, *28*, 5612.

(9) (a) Goldberg, D. E.; Harris, D. H.; Lappert, M. F.; Thomas, K. M. *J. Chem. Soc., Chem. Commun.* **1976**, *1976*, 261. (b) Leung, W. P.; Kwok, W. H.; Xue, F.; Mak, T. C. W. *J. Am. Chem. Soc.* **1997**, *119*, 1145. (c) Weidenbruch, M.; Stilter, A.; Marsmann, H.; Peters, K.; von Schnering, H. G. *Eur. J. Inorg. Chem.* **1998**, *1998*, 1333. (d) Eichler, B. E.; Power, P. P. *Inorg. Chem.* **2000**, *39*, 5444. (e) Leung, W.-P.; Cheng, H.; Huang, R.-B.; Yang, Q.-C.; Mak, T. C. W. *Chem. Commun.* **2000**, 451. (f) Stanciu, C.; Richards, A. F.; Power, P. P. *J. Am. Chem. Soc.* **2004**, *126*, 4106. (g) Rivard, E.; Fischer, R. C.; Wolf, R.; Peng, Y.; Merrill, W. A.; Schley, N. D.; Zhu, Z.; Pu, L.; Fettinger, J. C.; Teat, S. J.; Nowik, I.; Herber, R. H.; Takagi, N.; Nagase, S.; Power, P. P. *J. Am. Chem. Soc.* **2007**, *129*, 16197. (h) Lee, V. Y.; Sekiguchi, A. In *Organometallic Compounds of Low-Coordinate Si, Ge, Sn and Pb*; John Wiley & Sons, Ltd: Chichester, 2010; pp 199−334.

(10) Bleckmann, P.; Maly, H.; Minkwitz, R.; Neumann, W. P.; Watta, B.; Olbrich, G. *Tetrahedron Lett.* **1982**, *23*, 4655.

(11) (a) Becerra, R.; Boganov, S. E.; Egorov, M. P.; Faustov, V. I.; Krylova, I. V.; Nefedov, O. M.; Walsh, R. *J. Am. Chem. Soc.* **2002**, *124*, 7555. (b) Becerra, R.; Harrington, C. R.; Gaspar, P. P.; Leigh, W. J.; Vargas-Baca, I.; Walsh, R.; Zhou, D. *J. Am. Chem. Soc.* **2005**, *127*, 17469. (c) Boganov, S. E.; Egorov, M. P.; Faustov, V. I.; Krylova, I. V.; Nefedov, O. M.; Becerra, R.; Walsh, R. *Russ. Chem. Bull.* **2005**, *54*, 483.

(12) (a) Boatz, J. A.; Gordon, M. S.; Sita, L. R. *J. Phys. Chem.* **1990**, *94*, 5488. (b) Schoeller, W. W.; Schneider, R. *Chem. Ber.* **1997**, *130*, 1013. (c) Sakai, S. *Int. J. Quantum Chem.* **1998**, *70*, 291. (d) Su, M. D. *J. Phys. Chem. A* **2002**, *106*, 9563. (e) Oláh, J.; De Proft, F.; Veszprémi, T.; Geerlings, P. *J. Phys. Chem. A* **2004**, *108*, 490. (f) Su, M. D. *Chem. - Eur. J.* **2004**, *10*, 6073. (g) Tsai, M.-L.; Su, M.-D. *J. Phys. Chem. A* **2006**, *110*, 6216. (h) Lan, C.-Y.; Su, M.-D. *J. Phys. Chem. A* **2007**, *111*, 6232. (i) Broeckaert, L.; Geerlings, P.; Ruzicka, A.; Willem, R.; De Proft, F. *Organometallics* **2012**, *31*, 1605.

(13) Leigh, W. J.; Lollmahomed, F.; Harrington, C. R. *Organometallics* **2006**, *25*, 2055.

(14) Billone, P. S.; Beleznay, K.; Harrington, C. R.; Huck, L. A.; Leigh, W. J. *J. Am. Chem. Soc.* **2011**, *133*, 10523.

(15) Leigh, W. J.; Harrington, C. R.; Vargas-Baca, I. *J. Am. Chem. Soc.* **2004**, *126*, 16105.

(16) (a) Mathiasch, B. *Inorg. Nucl. Chem. Lett.* **1977**, *13*, 13. (b) Adams, S.; Dräger, M.; Mathiasch, B. *Z. Anorg. Allg. Chem.* **1986**, *532*, 81.

(17) (a) Fujiwara, H.; Sakai, F.; Sasaki, Y. *J. Chem. Soc., Perkin Trans. 2* **1983**, 11. (b) Yano, T.; Nakashima, K.; Otera, J.; Okawara, R.

Organometallics **1985**, *4*, 1501. (c) Beckmann, J.; Dakternieks, D.; Kuan, F. S.; Tiekink, E. R. T. *J. Organomet. Chem.* **2002**, *659*, 73.

(18) (a) Gibbons, A. J.; Sawyer, A. K.; Ross, A. *J. Org. Chem.* **1961**, *26*, 2304. (b) Sawyer, A. K.; Brown, Y. E.; Hanson, E. L. *J. Organomet. Chem.* **1965**, *3*, 464. (c) Davies, A. G. *J. Chem. Res.* **2004**, *2004*, 309.

(19) Murov, S. L.; Carmichael, I.; Hug, G. L. *Handbook of Photochemistry*, 2nd ed.; Dekker: New York, 1993; p 290.

(20) (a) Dakternieks, D.; Jurkschat, K.; van Dreumel, S.; Tiekink, E. R. T. *Inorg. Chem.* **1997**, *36*, 2023. (b) Davies, A. G. *Organotin Chemistry*, 2nd ed.; Wiley-VCH: New York, 2004; pp 186−189.

(21) Patel, Y.; George, J.; Pillai, S. M.; Munshi, P. *Green Chem.* **2009**, *11*, 1056.

(22) Our initial experiments employed a method of air purging that proved to be capable of removing only 60−70% of the dissolved oxygen in the air-saturated solvent.

(23) (a) Apodaca, P.; Cervantes-Lee, F.; Pannell, K. H. *Main Group Met. Chem.* **2001**, *24*, 597. (b) Kapoor, R. N.; Apodaca, P.; Montes, M.; Gomez, F. D.; Pannell, K. H. *Appl. Organomet. Chem.* **2005**, *19*, 518.

(24) The spikes in the absorbance−time profiles are attributed to thermal shock waves, generated by the release of a pulse of heat following absorption of the laser pulse by the solid particulate, which resonate back and forth through the cell. See: Scaiano, J. C. In *Reactive Intermediate Chemistry*; Moss, R. A., Platz, M. S., Jones, M., Jr., Eds.; John Wiley & Sons: New York, 2004; p 847.

(25) (a) Henning, J.; Eichele, K.; Fink, R. F.; Wesemann, L. *Organometallics* **2014**, *33*, 3904. (b) Wilfling, P.; Schittelkopf, K.; Flock, M.; Herber, R. H.; Power, P. P.; Fischer, R. C. *Organometallics* **2015**, *34*, 2222.

(26) (a) Tokitoh, N.; Ando, W. In *Reactive Intermediate Chemistry*; Moss, R. A.; Platz, M. S.; Jones, M., Jr., Eds.; John Wiley & Sons: New York, 2004; pp 651−715. (b) Moiseev, A. G.; Leigh, W. J. *Organometallics* **2007**, *26*, 6268. (c) Mizuhata, Y.; Sasamori, T.; Tokitoh, N. *Chem. Rev.* **2009**, *109*, 3479.

(27) Masamune, S.; Sita, L. R. *J. Am. Chem. Soc.* **1985**, *107*, 6390.

(28) Moiseev, A. G.; Leigh, W. J. *J. Am. Chem. Soc.* **2006**, *128*, 14442.

(29) (a) Trinquier, G. *J. Am. Chem. Soc.* **1990**, *112*, 2130. (b) Trinquier, G. *J. Am. Chem. Soc.* **1991**, *113*, 144.

(30) Drost, C.; Hildebrand, M.; Lonnecke, P. *Main Group Met. Chem.* **2002**, *25*, 93.

(31) (a) Lai, G.; Xu, Z.; Li, Z.; Jiang, J.; Kira, M.; Qiu, H. *Organometallics* **2009**, *28*, 3591. (b) Xu, Z.; Jin, J.; Li, Z.; Qiu, H.; Jiang, J.; Lai, G.; Kira, M. *Chem. - Eur. J.* **2009**, *15*, 8605. (c) Xu, Z.; Jin, J.; Zhang, H.; Li, Z.; Jiang, J.; Lai, G.; Kira, M. *Organometallics* **2011**, *30*, 3311.

(32) (a) Wintgens, V.; Johnston, L. J.; Scaiano, J. C. *J. Am. Chem. Soc.* **1988**, *110*, 511. (b) Carmichael, I.; Hug, G. L.; Scaiano, J. C. In *CRC Handbook of Organic Photochemistry*, Vol. *I*; CRC Press: Boca Raton, FL, 1989; pp 369−404.

(33) (a) Conlin, R. T.; Netto-Ferreira, J. C.; Zhang, S.; Scaiano, J. C. *Organometallics* **1990**, *9*, 1332. (b) Yamaji, M.; Hamanishi, K.; Takahashi, T.; Shizuka, H. *J. Photochem. Photobiol., A* **1994**, *81*, 1. (c) Kira, M.; Ishida, S.; Iwamoto, T.; Kabuto, C. *J. Am. Chem. Soc.* **1999**, *121*, 9722. (d) Tokitoh, N.; Kishikawa, K.; Okazaki, R.; Sasamori, T.; Nakata, N.; Takeda, N. *Polyhedron* **2002**, *21*, 563.

(34) The rate coefficient was measured at 540 nm, at which the extinction coefficient is roughly half the value at the absorption maximum (see Figure 5).

(35) (a) Leigh, W. J.; Lollmahomed, F.; Harrington, C. R.; McDonald, J. M. *Organometallics* **2006**, *25*, 5424. (b) Kostina, S. S.; Singh, T.; Leigh, W. J. *Organometallics* **2012**, *31*, 3755.

(36) Lollmahomed, F.; Huck, L. A.; Harrington, C. R.; Chitnis, S. S.; Leigh, W. J. *Organometallics* **2009**, *28*, 1484.

(37) Leigh, W. J.; Kostina, S. S.; Bhattacharya, A.; Moiseev, A. G. *Organometallics* **2010**, *29*, 662.

(38) Chai, J.-D.; Head-Gordon, M. *Phys. Chem. Chem. Phys.* **2008**, *10*, 6615.

(39) Check, C. E.; Faust, T. O.; Bailey, J. M.; Wright, B. J.; Gilbert, T. M.; Sunderlin, L. S. *J. Phys. Chem. A* **2001**, *105*, 8111.

(40) True minimum energy structures were successfully located for stannylstannylene **17b** using non-dispersion-corrected density functionals such as ωB97X or B3LYP.

(41) Boys, S. F.; Bernardi, F. *Mol. Phys.* **1970**, *19*, 553.

(42) Drost, C.; Hitchcock, P. B.; Lappert, M. F. *Angew. Chem., Int. Ed.* **1999**, *38*, 1113.

(43) The corresponding Hirshfeld charges at Sn^1 and Sn^2 in **20** are +0.21 and +0.45, respectively.

(44) Trinquier, G.; Malrieu, J. P. *J. Am. Chem. Soc.* **1991**, *113*, 8634.

(45) Chai, J.-D.; Head-Gordon, M. *J. Chem. Phys.* **2008**, *128*, 08410610.1063/1.2834918

(46) All of the $(SnPh_2)_2$ dimer structures located with the ωB97X(D) density functionals except for **20** were also identified as such at the B3LYP/LANL2DZ level of theory and exhibited similar relative energies to those found at the ωB97X/6-31+G(d,p)-LANL2DZdp level.

(47) Malcolm, N. O. J.; Gillespie, R. J.; Popelier, P. L. A. *Dalton Trans.* **2002**, *2002*, 3333.

(48) Fischer, R. C.; Power, P. P. *Chem. Rev.* **2010**, *110*, 3877.

(49) Alder, K.; Heimbach, K.; Neufang, K. *J. Liebigs Ann. Chem.* **1954**, *586*, 138.

(50) Rieke, R. D.; Xiong, G. *J. Org. Chem.* **1991**, *56*, 3109.

(51) Okawara, R.; Wada, M. *J. Organomet. Chem.* **1963**, *1*, 81.

(52) (a) Dräger, M.; Mathiasch, B.; Ross, L.; Ross, M. *Z. Anorg. Allg. Chem.* **1983**, *506*, 99. (b) Saito, M.; Okamoto, Y.; Yoshioka, M. *Appl. Organomet. Chem.* **2005**, *19*, 894.